A Basic Study on the Development of Ear-type Smart Monitor for Healthcare

Jihyoung Lee

February 2014

Dissertation

A Basic Study on the Development of Ear-type Smart Monitor for Healthcare

体調管理のためのイヤータイプ・スマート生体情報モニター開発を目指した基礎研究

Graduate School of Natural Science & Technology
Kanazawa University

Major subject: Innovative Technology and Science
Course: Intelligent System Creation

School registration No. 1123122214
Name: Jihyoung Lee
Chief advisor: Professor Shinobu Tanaka

Abstract

In the present study, I have proposed the development of "*ear-type smart monitor*" for healthcare in normal daily life. This novel system was designed for the simultaneous and continuous monitoring of the body core temperature, heart rate (HR) and normalized pulse volume (NPV; index of *a*-adrenalin-mediated sympathetic control at the finger arteriolar vessels) with the tailored ear-piece and smartphone. However, before the full-fledged development of prototype system, there have been several questions about methods of physiological index measurement. I have therefore performed four experiments.

As the result;

1) Newly developed tympanic thermometry using the tailored ear-piece could be used to the reliable body core temperature monitor in heat condition and during cycle ergometer exercise.
2) The green (530nm) light photoplethysmography (PPG) was more suitable measurement for monitoring of HR during motion than near-infrared (810nm), red (645nm) and blue (470nm) light PPG.
3) Theoretically, the final result in modified NPV equation (include light-scattering and absorption) was the same as original NPV equation (assumed non-scattering in the tissue). Experimentally, the reflection mode PPG and the transmission mode PPG were indeed the comparable method to derive NPV values.
4) The NPV derived from the bottom of the ear-canal with reflection mode PPG was found to be a valid measure when compared with reference measurements made in an index finger.

This paper discussed the issues related to these physiological index measurements.

Key-words: *ear-monitor, tympanic temperature, photoplethysmography, heart rate, normalized pulse volume.*

Acknowledgements

I would like to express the deeper appreciation to my chief advisors, Professor Shinobu Tanaka, Kanazawa University, Japan, and Professor Ken-ichi Yamakoshi, Showa University, Japan, for their valuable comments and excitement in regard to teaching, as well as for their kind help in research and scholarships. Especially, I would like to express the appreciation to my advisor, Ph. D. Takehiro Yamakoshi, Kanazawa University, Japan, for his guidance and persistent help in this research, as well as for his warm and kind assistance on my life abroad in Japan over 3years. Without talking to him, I would never have been able to pass through the sometimes dark moments of life abroad. Also, without their encouragement and tremendous support this research and my life abroad would not have been possible.

I would like to thank my advisor, Ph. D. Kenta Matsumura, Kanazawa University, Japan, for his insightful criticism and painstaking reading of my research, as well as encouragement and understanding always gave me great strength to continue. I also owe my sincere thanks to Professor Peter Rolfe, Harbin Institute of Technology, China, and OBH Ltd., UK., for his help in the difficult last stage of my paper writing and for his valuable comments. Special thanks go to Mr. Naoto Tanaka, Yusys Corp., Japan, and Professor Kyoungho Kim, Dankook University, Korea, for their encouragement and assistance.

In addition, greatest thank to Mrs. Yuriko Kawai, Ph. D. Yasuhiro Yamakoshi, Profesor Masamichi Nogawa, Ph. D. Kosuke Motoi, Ph. D. Mitsuhiro Ogawa, M.S. Yuki Itasaka, M.S. Shota Hanaki, M.S. Shimpei Miyazaki, and the laboratory's students in Kanazawa University.

Scholar fellowships (financial support) for the study abroad during 3years (from 2011 to 2013 year) were provided by the rotary yoneyama memorial foundation in Japan (2013), the JASSO in Japan (2012), and the Ishikawa prefecture in Japan (2011).

Finally, I would like to express the deeper appreciation to my family, Mr. Sangeok Lee, father, Mrs. Youngae Kim, mother, and Eunjung Lee, older sister.

Table of Contents

List of Figures

List of Tables

Abbreviations

mHealth: mobile health

eHealth: electronic health

$\boldsymbol{T}_c$: body core temperature

HR: heart rate

ECG: electrocardiography

PPG: photoelectric plethysmography (photoplethysmography)

PV: pulse volume

NPV: normalized pulse volume

mNPV: modified normalized pulse volume

NIR: near-infrared

LED: light emitting diode

PD: photodetector

ac: alternating-current

dc: direct-current

MPU: micro-processor unit

FFT: fast Fourier transform

SNR: signal-to-noise ratio

S.D.: standard derivation

S.E.M.: standard error of the mean

BL: baseline

HM: horizontal motion

VM: vertical motion

CPT: cold pressor test

dB: decibel

bpm: beats per minute

a.u.: arbitrary unit

HRt: HR derived from transmission mode PPG

HRr: HR derived from reflection mode PPG

PVt: PV derived from transmission mode PPG

PVr: PV derived from reflection mode PPG

$\boldsymbol{I}_{dc}$t: dc component derived from transmission mode PPG

$\boldsymbol{I}_{dc}$r: dc component derived from reflection mode PPG

NPVt: NPV derived from transmission mode PPG

NPVr: NPV derived from reflection mode PPG

IF: index finger

ECT: the top of ear-canal

ECB: the bottom of ear-canal

EAU: the upper part of ear-auricle

EAL: the lower part of ear-auricle

Chapter I.

Introduction

1.1. Motivation

1.1.1. Climate and Health

There have been several studies examining adverse health effects (include deaths) related to the climate change as the extreme weather events [1-3]. Extreme weather events include the period of very high temperature (heat waves and extreme summer conditions) and very low temperature (cold waves and extreme winter conditions). These extreme temperatures not only trigger heatstroke, but also exacerbate many pre-existing health problems, leading to elevated mortality rates [4]. Figure 1.1 shows the mortality by the extreme temperatures over the world. Particularly, deaths related to the heat stroke in period of extreme summer have become the serious societal problem around the world [5]. Data on the EM-DAT (International disaster database supported by United States Agency for International Development; http://www.emdat.be) show that at the 2003 and 2010, over 70,000 and 50,000 deaths by heat waves, respectively, over the world. Also, in the some other northern high latitude countries, seasonal death rates and illness events are higher in winter than in summer [1]. The incidence of the deaths by extreme weather events may increase with global warming and the predicted worldwide increase in the frequency and intensity of extreme weather events [5]. Early

planning can help reduce future mortality, for example the emergency management and public health prevention, can improve health by addressing climate change [2].

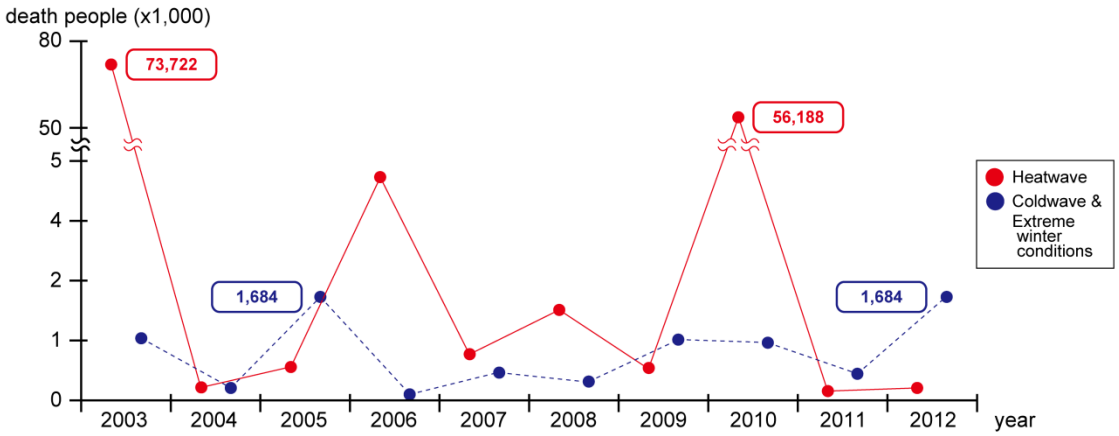

Figure 1.1 Extreme temperatures related mortality over the world.

1.1.2. Advanced Technologies for Healthcare

Recently, academic researchers and healthcare industrial are actively developing compact measurements, low-cost technologies for convenient and effective health screening, monitoring and personalized healthcare [6-8]. Particularly, mobile health (mHealth or m-health) is regarded as a central element for the healthcare in normal daily life. The mHealth is a part of electronic health (eHealth) and is the provision of health service and information by using mobile communication devices such as smartphone and PDAs [6]. Figure 1.2 shows the schematic drawing for mHealth applications.

The mHealth applications include collection of clinical health data, delivery of healthcare information to general users, researchers and patients, as well as handy bioinstrumentation for real-time monitoring of patient vital signs, and direct provision of care *via* mobile communication devices [6]. The mHealth field could also make key contributions to point-of-care testing, which is now of widespread interest as a component of emerging clinical medicine. Rapid advances in the field of mHealth strongly depend on significant recent progress in information and communication technology, which of course includes mobile communication technologies [6]. The advanced technologies for healthcare include the convenience measurement for long-term monitoring [7], point-of-care analyzing and testing using smartphone [6], wearable

body sensor networks [9] and non-invasive physiological variables monitoring instruments [10].

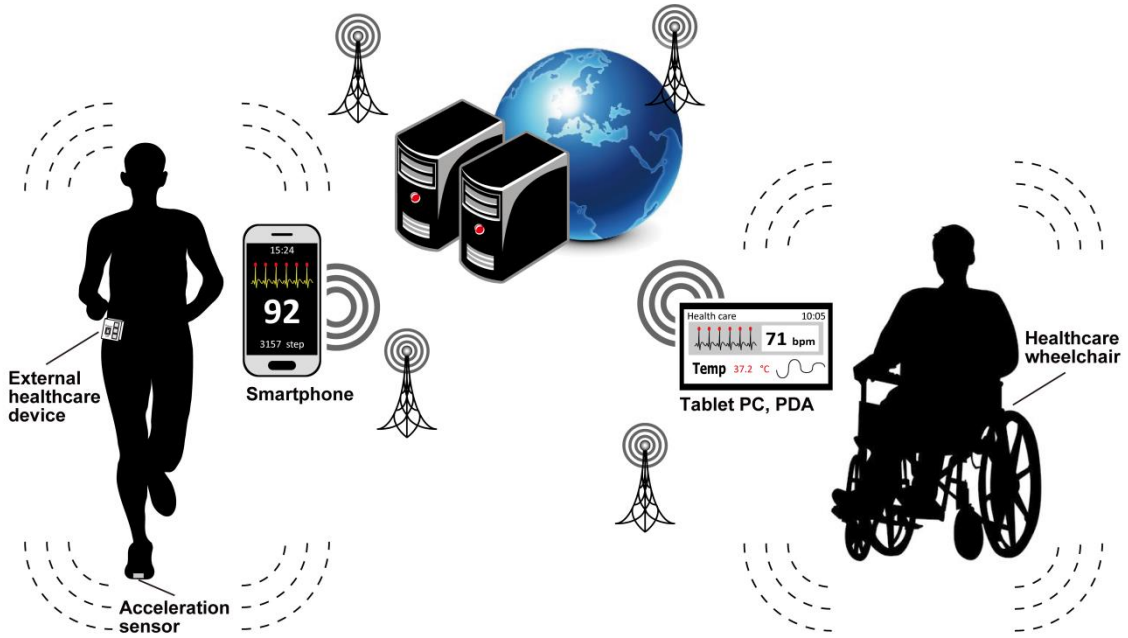

Figure 1.2 The schematic drawing for mHealth system.

1.2. Related Studies

There have been sustained efforts, over recent decades, to develop and improve non-invasive methods to monitor physiological variables in various circumstances and such methods are of importance for clinical diagnosis and for monitoring therapies, as well as for research [9-12]. Non-invasive measurement is generally considered to be most desirable approach for practical use, but in addition there is a significant increasing need to monitor physiological variables in a manner that allows the subject to be unconstrained, which can be achieved by the so-called ambulatory or wearable monitoring techniques [9]. The development of wearable techniques using finger ring [13], wrist band [14, 15] and ear-clip [16] have also attracted considerable interest. Particularly, the around ear has the internal carotid and superficial temporal artery with theirs branches supply [17-19]. This site is useful for studying plethysmogram and

tympanic temperature. For example, as the interesting ear-type application for healthcare, Poh *et al.* [16] developed a wearable photoplethysmographic sensor with wireless networking to monitor the heart rate derived from photo-pulsation using the ear-clip. The portable ear thermometer, which uses infrared radiation measurement, is becoming popular. Many studies have shown that the accuracies of most ear thermometers are acceptable for ordinary clinical setting use [11]. However, these previous measurements have several limits. The portable ear thermometer did not measure temperature continuously, which makes it unsuitable for continuous measurement in normal daily life and during exercise [20]. The ear-clip photoplethysmographic sensor measures the pulsation at the external part of ear (ear-lobe) [16]. So, it may be affected by the ambient light in the uncontrolled environment as the outdoor.

1.3. Proposed the Ear-type Smart Monitor

I have proposed the novel ear-type physiological variables monitor based on the mHealth technologies, which I call "*ear-type smart monitor*". This system includes the wearable tailored ear-piece and smartphone.

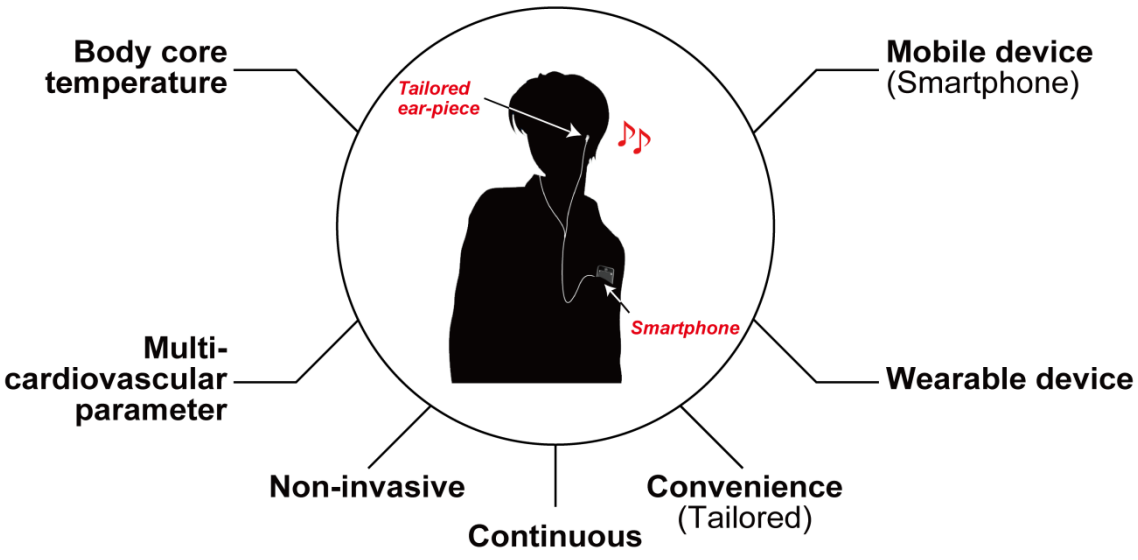

Figure 1.3 The concept of ear-type smart monitor.

Figure 1.3 shows the concept of ear-type smart monitor. This system features the non-invasive, convenient and continuous monitoring of physiological variables including the body core temperature and cardiovascular parameter. Briefly, physiological variables are taken from the ear *via* tailored ear-piece, and then transmitted to the smartphone. The smartphone provides the point-of-care testing based on the received physiological variables. Particularly, the tailored ear-piece for individual's ear might be capable of improving the accuracy of physiological variable measure. The smartphone might be capable of real-time analysis, transmission and record.

Chapter II.

Introduction of Physiological Variables

2.1. Body Core Temperature

The body core temperature (T_c) is an important physiological index of thermal strain in the body. T_c is essentially the temperature of blood in the pulmonary artery, but measurement of intra-pulmonary arterial temperature is invasive method [20, 21]. Esophageal temperature has been preferred by some as the most representative of T_c, especially during thermal transients [22, 23]. However, esophageal temperature has not gained wide acceptance because of technical difficulties and discomfort associated with placement of an esophageal probe [23]. Besides that, the alternative measurement of T_c, there are several body sites that indirectly reflect core temperature, examples including rectum, gastrointestinal tract, axillary, oral, tympanic [20], and highly-insulated skin temperature [24]. Table 2.1 summarizes the T_c measurements.

Of all of these possible measurements, considering the need to make measurements non-invasively and conveniently without undue encumbrance to the user in normal daily life, the measurement of tympanic temperature would appear to be the most appropriate technique in practice. In addition, it has been reported that tympanic temperature is the most reliable non-invasive index of T_c, for the reason that the eardrum reflects the temperature of the internal carotid artery, which feeds the hypothalamus [25, 26]. Sato

et al. [23] reported that the tympanic temperature by contact method using a thermocouple truly reflects the T_c The non-contact tympanic temperature by infrared method using an optical fiber has been shown to accurately reflect the esophagus temperature during the heat stress and exercise [27]. Moreover, the infrared ear thermometers are extensively used for measuring the temperature of a human body in the clinical [21], sports science [28-31] and normal daily life. Figure 2.1 shows the tympanic temperature measurement using infrared ear thermometer.

Table 2.1 The body core temperature (T_c) measurements.

Body site	Method	Measurement
Intra-pulmonary Arterial	Invasive	Thermistor
Esophagus	Invasive	Thermistor
Rectal	Invasive	Thermistor
Axilla	Non-invasive	Thermistor
Sublingual (Oral)	Non-invasive	Thermistor
Skin surface	Non-invasive	Zero-heat-flow or Dual-heat-flux thermometer
Tympanic (Ear)	Non-invasive	Thermistor or Infrared thermometer
Gastrointestinal	Non-invasive	Ingestible telemetry pill

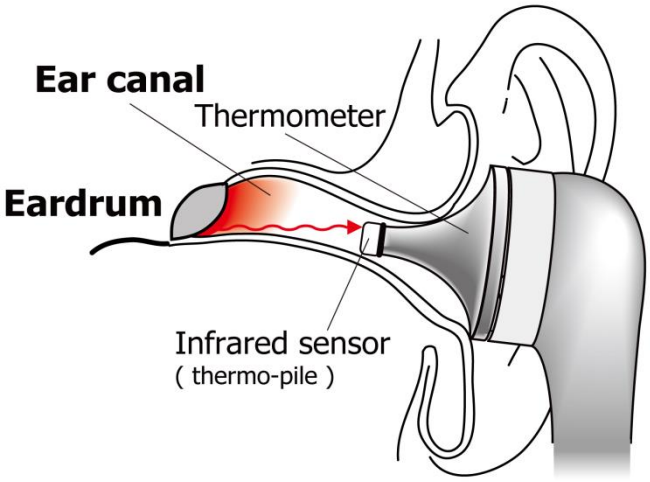

Figure 2.1 The tympanic temperature measurement using infrared ear thermometer.

2.2. Heart Rate

The heart rate (HR) is an important physiological parameter to measure for clinical diagnosis and for monitoring therapies, as well as for physiological research [32]. HR is essentially based on the heart beat signals, which could be taken from the QRS complex or the R waves derived from electrocardiography (ECG), or the pulse waves derived from plethysmography [32, 33]. The plethysmogram can be measured quantitatively or detected qualitatively with a number of techniques, including air or water plethysmography, strain gauge plethysmography, electrical impedance plethysmography and photoelectric plethysmography (PPG) [34, 35]. Particularly, PPG is a popular optical technology for the monitoring HR in normal daily life due to its simplicity and convenience, in its simplest form only requiring the attachment of a light emitting diode (LED) and a photodetector (PD) [36]. PPG has been shown to be capable of providing accurate quantitative data for HR even under challenging conditions [37, 38]. Figure 2.2 shows the ECC and PPG waveforms. One approach, to determine the HR from photoplethysmogram, can be the calculation of inter-beat interval (e.g. peak-to-peak interval of photoplethysmogram). The inter-beat interval is the time interval between individual beats of the heart. The HR is typically expressed as beats per minute (bpm).

That is, HR could be derived simply by inter-beat interval, giving the following relationship:

$$\text{HR [bpm]} = \left(\frac{60}{\text{Inter - beat interval}} \right)$$

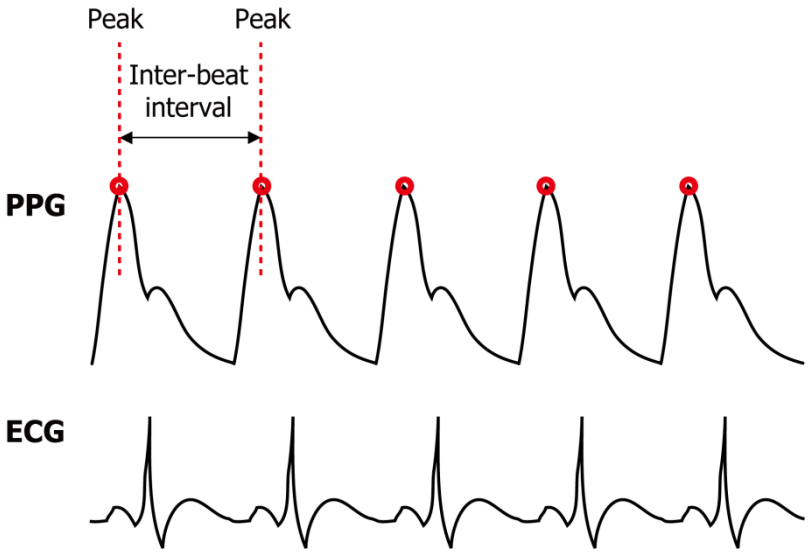

Figure 2.2 The electrocardiography (ECC) and photoplethysmography (PPG) waveforms.

Traditionally, the photoplethysmogram has been obtained from the fingertip with the near-infrared (NIR) light source and detector in the transmission configuration. This site is particularly useful for studying PPG since the arteriolar vessels here are known to be very rich. Other anatomical sites have also been used, in some cases, such as the toe and ear lobe, with transmittance configuration and in other cases, including the forehead and esophagus, using the reflectance configuration [32, 39]. Of all of these possible sites, the different locations on and in the ear-canal can have several advantages [40-42].

1) relatively free from motion artifacts and orthostatic pressure modulation, as the head is less affected by motion than the other extremities as a finger and toe; and

2) less impairment from low perfusion because the many blood vessels are very close to the lining and periphery of the ear-canal.

Vogel *et al.* [41] have validated the measurement of HR derived from the ear-canal using the PPG during motion. Figure 2.3 shows the PPG at the ear-canal with the ear-piece.

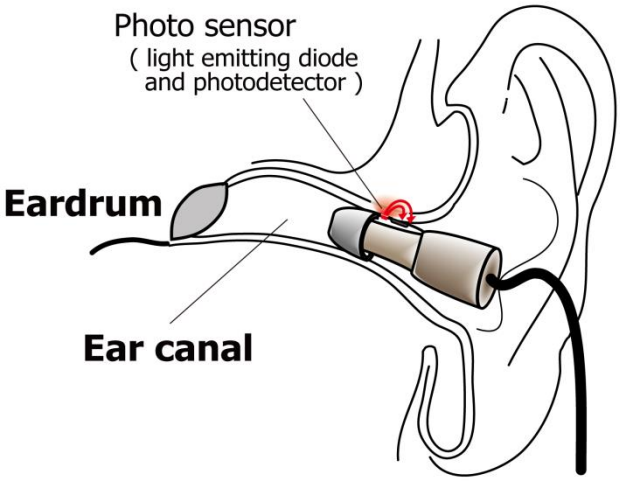

Figure 2.3 The photoplethysmography (PPG) at the ear-canal with the ear-piece.

2.3. Normalized Pulse Volume

Recent studies have been reported that suggest that normalized pulse volume (NPV) is a superior index derived from the finger transmission mode PPG waveform for the assessment of α-adrenergically mediated vascular tone [43].

Signals produced by PPG relate to the intensity of light, $\boldsymbol{I}$, that is detected following absorption and scattering processes as the incident light, $\boldsymbol{I}_o$, propagates within tissues, and the Beer–Lambert–Bouguer law can be used to describe the relationship between $\boldsymbol{I}$ and $\boldsymbol{I}_o$.

$$-ln\left(\boldsymbol{I}/\boldsymbol{I}_o\right) = \varepsilon CV \ . \qquad (2.1)$$

The PPG signal, which arises from $\boldsymbol{I}$, contains two basic components: firstly, a cardiac synchronous pulse, the alternating-current (ac) component, $\boldsymbol{I}_{ac}$, which is

produced by the absorption of light by pulsating arterial and arteriolar blood; secondly, a slowly varying background signal, the direct-current (dc) component, $\boldsymbol{I}_{\mathrm{dc}}$, that is related to absorption of light by tissues and venous blood. Figure 2.4 shows two component of PPG signal. The pulse volume (PV) signal derived from $\boldsymbol{I}$ in this way certainly has a relationship with the true arterial PV in the region of tissue interrogated by the light emitter–detector pair, but the exact relationship varies according to a number of factors, including the emitter–detector spacing and configuration, the wavelength of light used and the anatomical site used for the measurement. Thus direct comparisons of PV signals between different sites and different subjects are not possible. In order to address this problem, at least in part, the very earliest reports of the method included approaches for the normalization of the PV-related plethysmogram signals, that is the ac component, for example by expressing the volume pulse amplitude, $\boldsymbol{I}_{\mathrm{ac}}$, as a percentage of the total photoelectric signal, $\boldsymbol{I}$; thus normalized pulse volume, NPV, was calculated as ($\boldsymbol{I}_{\mathrm{ac}}/\boldsymbol{I}$) 100% [44]. The total photoelectric signal, $\boldsymbol{I}$, is often rewritten as $\boldsymbol{I}_{\mathrm{dc}}$ and this is a valid approximation since $\boldsymbol{I}_{\mathrm{ac}}$ is very much smaller than $\boldsymbol{I}_{\mathrm{dc}}$. Further approaches are to normalize the $\boldsymbol{I}_{\mathrm{ac}}$ amplitude to the baseline $\boldsymbol{I}_{\mathrm{ac}}$ amplitude, or to the dc component, $\boldsymbol{I}_{\mathrm{dc}}$, [43, 45, 46] or, to enable waveform changes to be perceived more easily, to normalize the $\boldsymbol{I}_{\mathrm{ac}}$ pulse width to the baseline pulse width value [47].

That is, NPV could be derived simply by normalizing the amplitude of the ac component to the mean dc component, giving the following relationship [43]:

$$\mathrm{NPV} = \Delta \boldsymbol{I}_{\mathrm{ac}} / \boldsymbol{I}_{\mathrm{dc}} \left(\propto \Delta V_a \right). \tag{2.2}$$

This equation (2.2) is described dividing the ordinal PV ($\Delta \boldsymbol{I}_{\mathrm{ac}}$) as the peak to foot amplitude of the ac component by the intensity of transmitted light ($\boldsymbol{I}_{\mathrm{dc}}$) as the mean dc component photoplethysmographically detected from the finger. Namely, NPV denoted the pulsatile change in the arterial blood volume, ΔV_a [43].

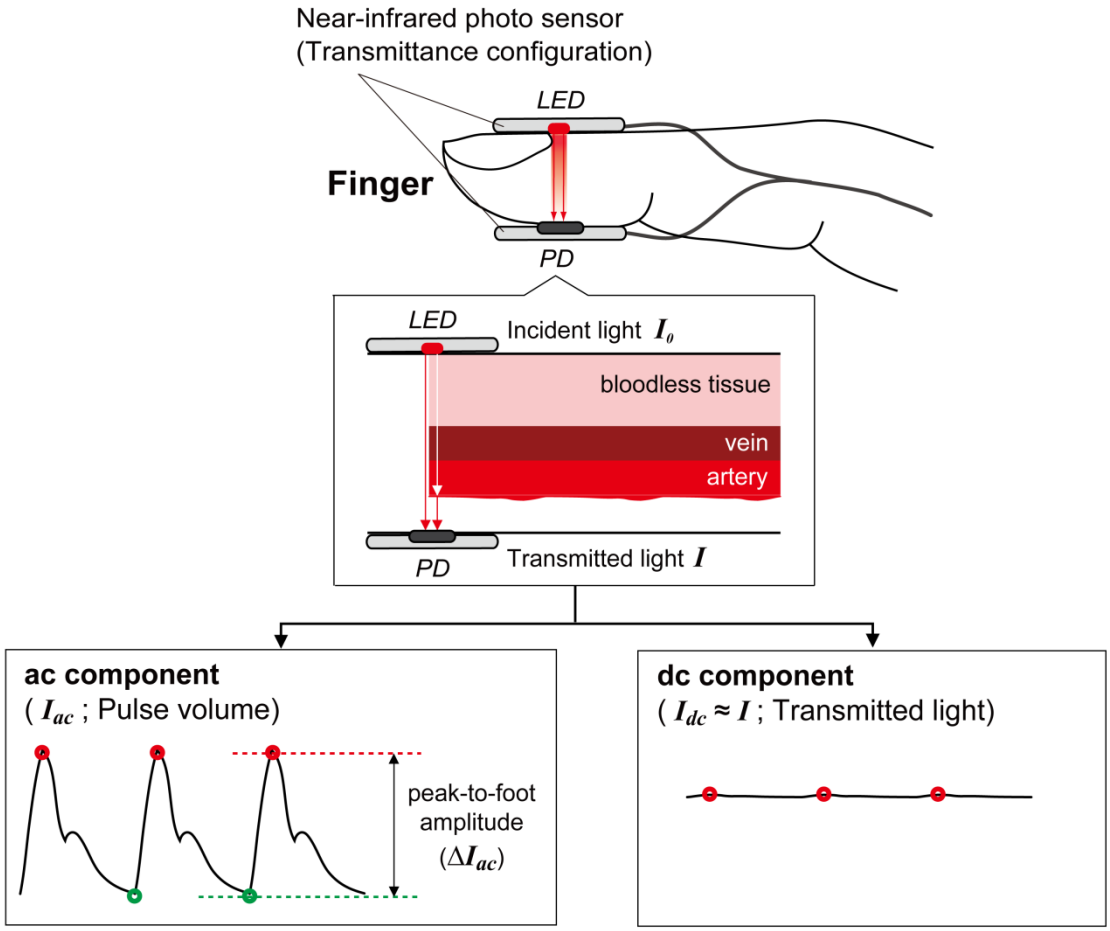

Figure 2.4 Two component of photoplethysmography (PPG) signal.

Chapter III.

Objectives

3.1. Design of Ear-type Smart Monitor

In this chapter, I have designed the "*ear-type smart monitor*", specifically. Figure 3.1 shows the schematic of ear-type smart monitor. The whole system includes the two main applications: 1) the *tailored ear-piece* to measure of various physiological variables; and 2) the *smartphone* to monitor and data analyzing. The central element of the system is the newly developed ear-piece, tailored ear-piece, with the custom-made to incorporate an infrared temperature and photo sensors. Particularly, the tailored ear-piece for individual's ear is designed for the accurate measurement of the tympanic temperature and photo-plethysmogram.

The tympanic temperature was measured using the infrared temperature sensor as a thermopile. The photo-plethysmogram, which is the peripheral pulse volume obtained by the photo sensor, is taken from around inner ear skin. The measured signals are transmitted to the smartphone. And then, calculated: 1) $\boldsymbol{T}_c$ [30]; 2) HR [32] derived from the photo-plethysmogram; and 3) NPV [43] derived from the photo-plethysmogram. Moreover, the smartphone provides the point-of-care testing *via* application as the *iPhysioMeter* [48].

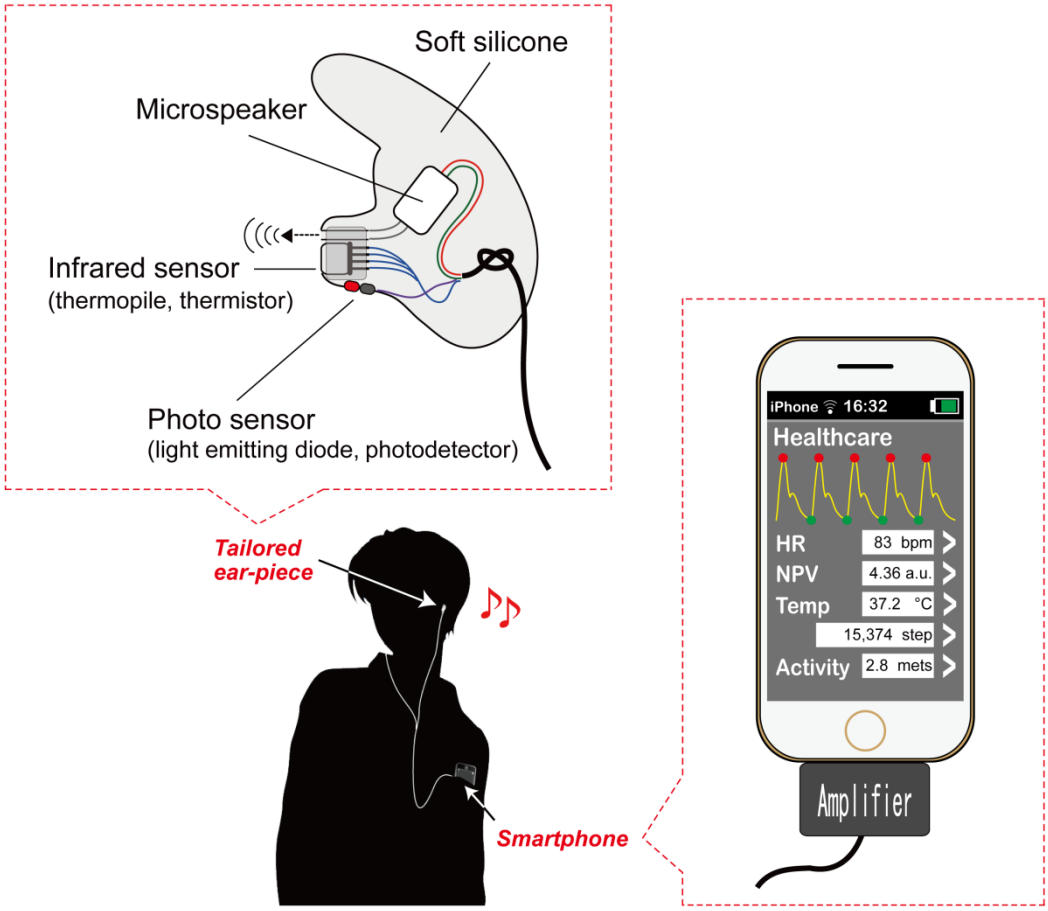

Figure 3.1 The schematic of ear-type smart monitor.

3.2. Objectives

In the present study, the final goal was the development of the "*ear-type smart monitor*" for healthcare in normal daily life. However, before the development of prototype of ear-type smart monitor, there have been several questioned for the physiological variables measurement.

1) ***Reliability of non-contact tympanic temperature measurement***: Many studies have reported that the non-contact tympanic temperature measurement is acceptable method for T_c monitoring in the clinical setting [11]. On the other hand, in some studies, the reliable use of tympanic temperature during heat

stress and exercising has been seriously questioned [28, 49-51]. In addition, to the best of my knowledge, there is no convenient device for the continuous monitoring of tympanic temperature. Therefore, I have developed a variant of this having certain novel features that make it particularly suitable for reliable and continuous monitoring. The purpose of this experiment was to examine the novel tympanic temperature measurement method using the tailored ear-piece and an infrared-radiation-sensor for continuous monitoring [29-31].

2) ***Most suitable PPG light color for HR monitoring during motion***: PPG is a popular optical technology for the monitoring heart rate HR in normal daily life due to its simplicity and convenience [32]. However, the reliability of PPG signals measured during normal daily life can be reduced by motion artifacts [32]. One approach for the robust measurement of PPG signals during motion, based on the optical characteristics of tissue, can be the choice of light wavelength [52-54]. Particularly, among the possible light colors of PPG, green light PPG has been shown to have the least influence from motion artifacts when compared with the NIR light PPG [52]. However, despite the possible advantages of green light PPG, in terms of susceptibility to artifact little is known about the accuracy of HR measured by green light PPG during motion. Therefore, the purpose of this experiment was to discover the most suitable light color of PPG for measuring HR during normal daily life, where motion is likely to be a significant issue [55].

3) ***Modified normalized pulse volume***: The transmission PPG obtained from a finger to derive the NPV has been analyzed theoretically with the application of the Beer-Lambert-Bouguer law [43]. However, the validity of original NPV must be questioned since it is based on the assumption of a non-scattering medium (*cf*. Original NPV is not valid for the reflection mode PPG due to non-scattering assumption); in fact, when light passes through biological tissues it is extensively scattered as well as absorbed. The modified Beer-Lambert-Bouguer law, which includes the influence of light-scattering, should be considered [56-58]. Furthermore, the method for measuring ear-photoplrthysmogram with the

tailored ear-piece is based on the reflection mode PPG. Therefore, the purpose of this experiment was to derive the modified NPV (mNPV; valid for the transmission mode PPG as well as reflection mode PPG) theoretical relationship in real biological tissues, and to validate the mNPV experimentally using transmission and reflection mode PPG [59].

4) ***Ear normalized pulse volume***: Traditionally, the photoplethysmogram has been obtained from the fingertip. Several anatomical sites have been used, in some cases, such as the toe and ear lobe, with transmission optodes and in other cases, including the forehead and esophagus, using the reflectance configuration [32]. Of all of these possible sites, the different locations on and in the ear can have several advantages (close with the blood vessels and relative freedom from motion artifacts) [41]. Despite advantages, the NPV derived from the ear has not yet been validated. Furthermore, the most suitable location around the ear for the robust measurement of PPG signals using tailored ear-piece has not yet been examined. Therefore, the purpose of this experiment was to discover the most suitable location for obtaining robust ear PPG signal, and to validate the ear NPV [59].

I have performed four experiments about the physiological variables measurement.

Chapter IV.

Experiments and Results

4.1. Reliability of Non-contact Tympanic Temperature Measurement

4.1.1. Introduction

The tympanic temperature measurement has been widely used to monitor of $\boldsymbol{T}_c$ [60]. Many studies have shown that the accuracies of most infrared ear thermometers are acceptable for ordinary clinical setting use. In addition, the measurement of tympanic temperature would appear to be the most appropriate technique for continuous monitoring of $\boldsymbol{T}_c$. However, the reliable use of tympanic temperature as an index of $\boldsymbol{T}_c$ during heat stress and exercising has been seriously questioned. For example, Nielsen [49], Deschamps *et al.* [50], Easton *et al.* [51], and Casa *et al.* [28] reported that the tympanic temperature was lower than $\boldsymbol{T}_c$ (ef. esophageal and rectal temperature) during exercise due to the influence of ambient temperature. On the other hand, Mariak *et al.* [26] reported that the tympanic temperature reflects cerebral temperature. Newsham *et al.* [61] reported no differences between peak tympanic temperature and rectal temperature on cessation of exercise, although tympanic temperature increased to a greater extent than rectal temperature.

Therefore, although the non-contact tympanic temperature measurement is an established method [27], I have developed a variant of this having certain novel features

that make it particularly suitable for reliable and continuous monitoring. The device allows tympanic temperature monitoring based on an infrared-radiation-type method, which I call "*tailored ear-piece tympanic thermometry*" [29-31]. Especially, this method employs a tailor-made ear-piece which effectively achieves a hermetically sealed condition. The purpose of the present study was to examine the reliability of the developed system for continuous tympanic temperature monitoring. Firstly, under controlled heat conditions, I compared measurements from the new system with the contact tympanic temperature and the gastrointestinal temperature as gold-standard references of $\boldsymbol{T}_c$ [31]. Next, I compared those during cycle ergometer exercise.

4.1.2. Experimental Method

4.1.2.1. Participants

Ten healthy male participants, with a mean age of 22.9 ± 1.9 standard derivation (S.D.) years, without known cardiovascular disorders participated in the present study. All participants agreed to take part in this study voluntarily and signed an informed consent statement. The experimental design was approved by the ethics committee of the Kanazawa University.

4.1.2.2. Measurements

I used a micro-miniature thermo-pile sensor (10TP583T, Ishizuka Elec. Corp.: 5φ) for non-contact measure of tympanic temperature. The electrical signals from the thermo-pile element and the thermistor element (LM35, National Semiconductor Japan Co., Ltd.) situated in the amplifier unit are fed to the main unit. The arithmetic processing of the temperatures is executed by a calibration program installed in the micro-processor unit (MPU) (dsPIC30F5011-30I, Microchip Technology Japan Co., Ltd.) of the main unit. Temperature and time data are then recorded in the SD memory. Inclusion of a memory function on an SD memory card, which can continuously output the data at the set sampling interval. In order to calibrate the thermo-pile sensor I have used a blackbody furnace (Thermometer comparator, Elec. Temp. Instruments Ltd.), and a reference thermometer (Reference Thermometer, Elec. Temp. Instruments Ltd.:

accuracy ± 0.2 °C, resolution 0.1 °C). Firstly, I determined the coefficient of the calibration curve from the digital value obtained by an A/D converter, which was measured in 2 °C steps from 34 °C to 44°C. Then, I stored the coefficient value in the MPU and the sensor signals are thereby converted into the measured temperature values.

Moreover, I used three electronic thermometers (DS103, TECHNOL SEVEN Co., Ltd.: accuracy ± 0.02 °C, resolution 0.001 °C) with three highly sensitive thermistor probes (SXK-67 & SZL-64, TECHNOL SEVEN Co., Ltd.: 3φ), which were properly calibrated at fixed temperatures specified in the International Temperature Scale of 1990 (ITS-90) by the manufacturer who provided a test chart just before the experiment. One of these probes was inserted into the ear canal for direct measurement of tympanic temperature. The thermo-pile infrared tympanic thermometer under evaluation was inserted into the contra-lateral ear canal. In addition, I used a CorTempTM telemetry pill sensor (12φ*20 mm; CorTemp, HQ Inc., USA: accuracy ± 0.1 °C, resolution 0.01 °C) for measurement of gastrointestinal temperature [20, 51, 62]. The measured temperatures were recorded at 30 s intervals, which is sufficient to follow the relatively slow changes that can occur in core temperature.

Figure 4.1 shows the attachment configurations of the non-contact and the contact body temperature sensors. As is seen here I positioned the tailor-made ear-piece with the implanted thermo-pile sensor in the right ear. In the left ear I carefully placed the thermistor probe so as to softly contact the eardrum, and then fixed it by infusing an impression material (detax addition, DETAX GmbH & Co. KG, Germany). This was carried out under the supervision of a doctor. Thermistor probes of the same type were used for the measurement of ambient and water bath temperatures, and these were fixed around the participants and to the inside wall of the bathtub respectively.

4.1.2.3. Experimental Design

Tests were performed during one week. On each of the test days, participants ingested a telemetry pill sensor 3 hour prior to the experiment. After ensuring that the participants had adequate hydration with appropriate fluid intake 1 hour before the experiment, they were requested to sit down in a quiet, temperature-controlled, healthcare laboratory having a built-in bathroom, in Kanazawa University.

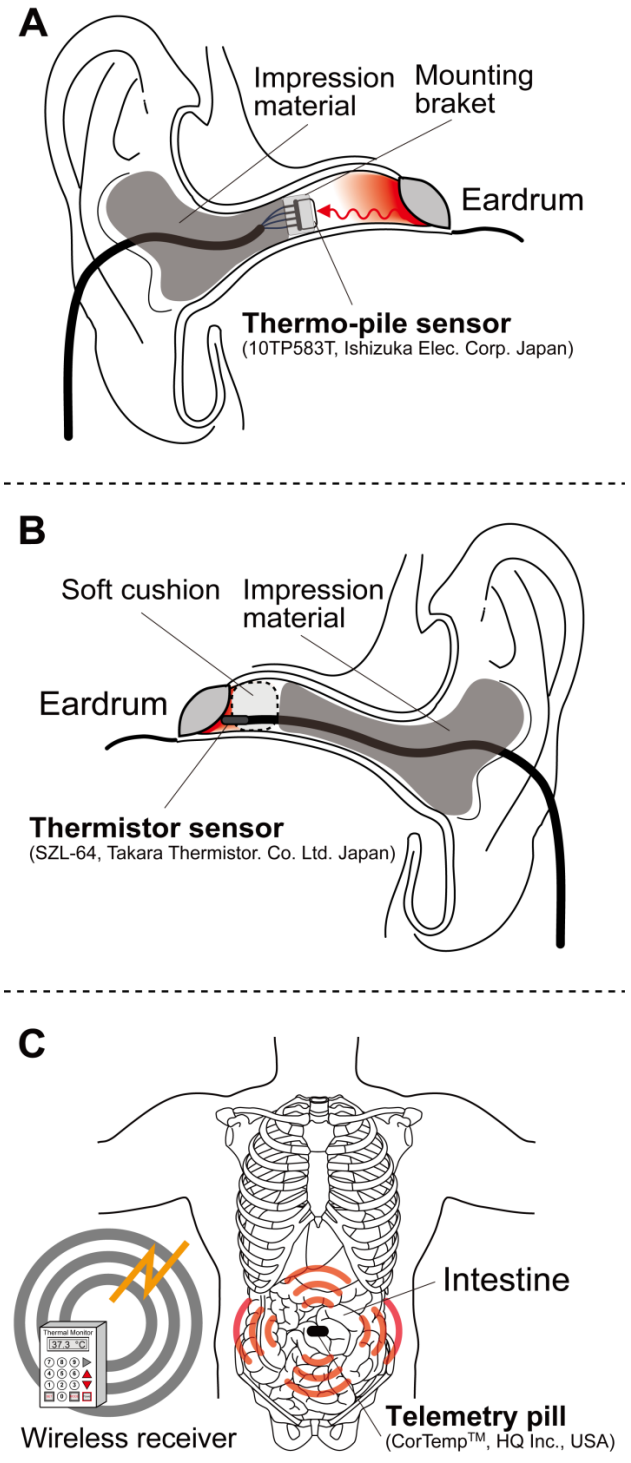

Figure 4.1 Attachment configurations of body temperature sensors [31]. (A) Left-side ear; the non-contact sensor (thermo-pile) for tympanic temperature. (B) Right-side ear; the contact sensor (thermistor) for tympanic temperature as a reference. (C) Stomach; the telemetry pill sensor for gastrointestinal temperature as a reference of body core temperature.

The six stages of the experiment were carried out in the following order: (a) each volunteer wore a bathing suit and had the temperature sensors attached in the appropriate positions; (b) a rest period of 10 min; (c) a bathing period of 30 min, with the water preset to 42 °C; (d) a 40 min period during which the body temperature was reduced gradually by natural cooling in the laboratory; (e) the cycle ergometer exercise period of 40 min; (f) a 20 min period during which the body temperature was reduced gradually by natural cooling in the laboratory. The test was performed over a 140 min period.

4.1.2.4. Data Analyses

I used Pearson's correlation analysis and *Bland-Altman* plots for assessing the differences between the two measuring methods [63].

4.1.3. Results

4.1.3.1. Agreements in heat condition

Figure 4.2 shows the relationships between the contact-type tympanic temperature ($\boldsymbol{T}_{\text{ty-contact}}$) and the tympanic temperature measured by the proposed method ($\boldsymbol{T}_{\text{ty}}$) and, between the gastrointestinal temperature ($\boldsymbol{T}_{\text{gi}}$) and $\boldsymbol{T}_{\text{ty}}$ (see figure 4.2 panel A). Their corresponding *Bland-Altman* plots are shown in figure 4.2 panel B. These results demonstrate a strong correlation between the $\boldsymbol{T}_{\text{ty}}$ and both the $\boldsymbol{T}_{\text{ty-contact}}$ (r = 0.99, n = 1400, P < 0.001) and the $\boldsymbol{T}_{\text{gi}}$ (r = 0.93, n = 1400, P < 0.001). According to the *Bland-Altman* analysis, the mean difference between these temperatures ($\boldsymbol{T}_{\text{ty}} - \boldsymbol{T}_{\text{ty-contact}}$, $\boldsymbol{T}_{\text{ty}} - \boldsymbol{T}_{\text{gi}}$) was +0.01 °C, +0.27 °C, and limits of agreement were ± 0.30 °C, ± 0.58 °C, respectively [31].

4.1.3.2. Agreements during cycle ergometer exercise

Figure 4.3 shows the relationships between $\boldsymbol{T}_{\text{ty-contact}}$ and the tympanic temperature measured by $\boldsymbol{T}_{\text{ty}}$ and, between $\boldsymbol{T}_{\text{gi}}$ and $\boldsymbol{T}_{\text{ty}}$ (see figure 4.3 panel A). Their corresponding *Bland-Altman* plots are shown in figure 4.3 panel B. These results demonstrate a strong correlation between the $\boldsymbol{T}_{\text{ty}}$ and both the $\boldsymbol{T}_{\text{ty-contact}}$ (r = 0.94, n = 1190, P < 0.001) and the

T_{gi} (r = 0.90, n = 1400, P < 0.001). According to the *Bland-Altman* analysis, the mean difference between these temperatures ($T_{ty} - T_{ty\text{-}contact}$, $T_{ty} - T_{gi}$) was –0.04 °C, +0.37 °C, and limits of agreement were ± 0.28 °C, ± 0.37 °C, respectively.

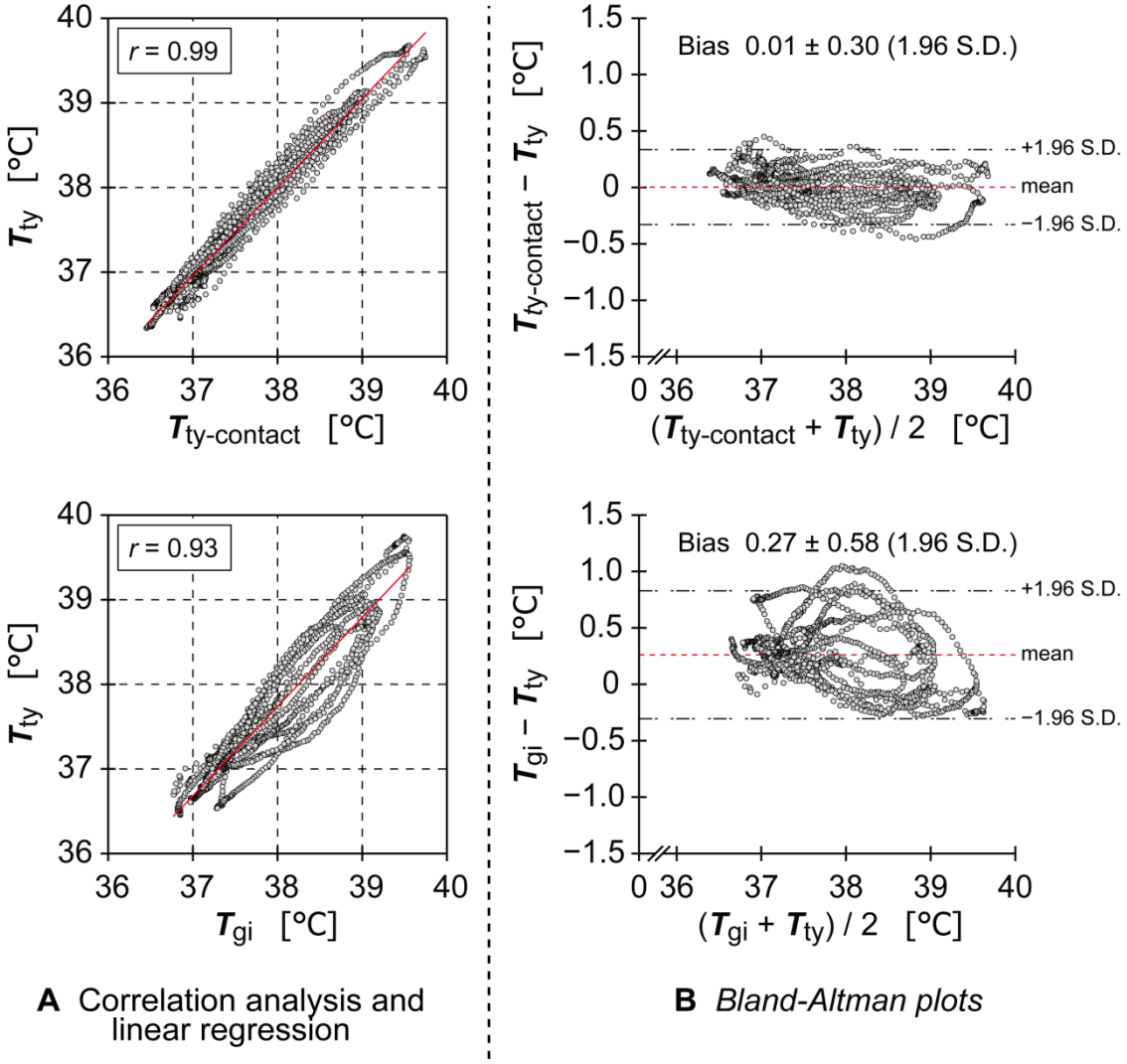

Figure 4.2 Statistical analysis results of comparative evaluation test in the heat condition [31]. (A) The scatter plot for Pearson's correlation analysis and the linear regression between the contact tympanic temperature ($T_{ty\text{-}contact}$) and the non-contact tympanic temperature measured by the present system (T_{ty}), and that between the gastrointestinal temperature (T_{gi}) and T_{ty}, and (B) their *Bland-Altman* plots.

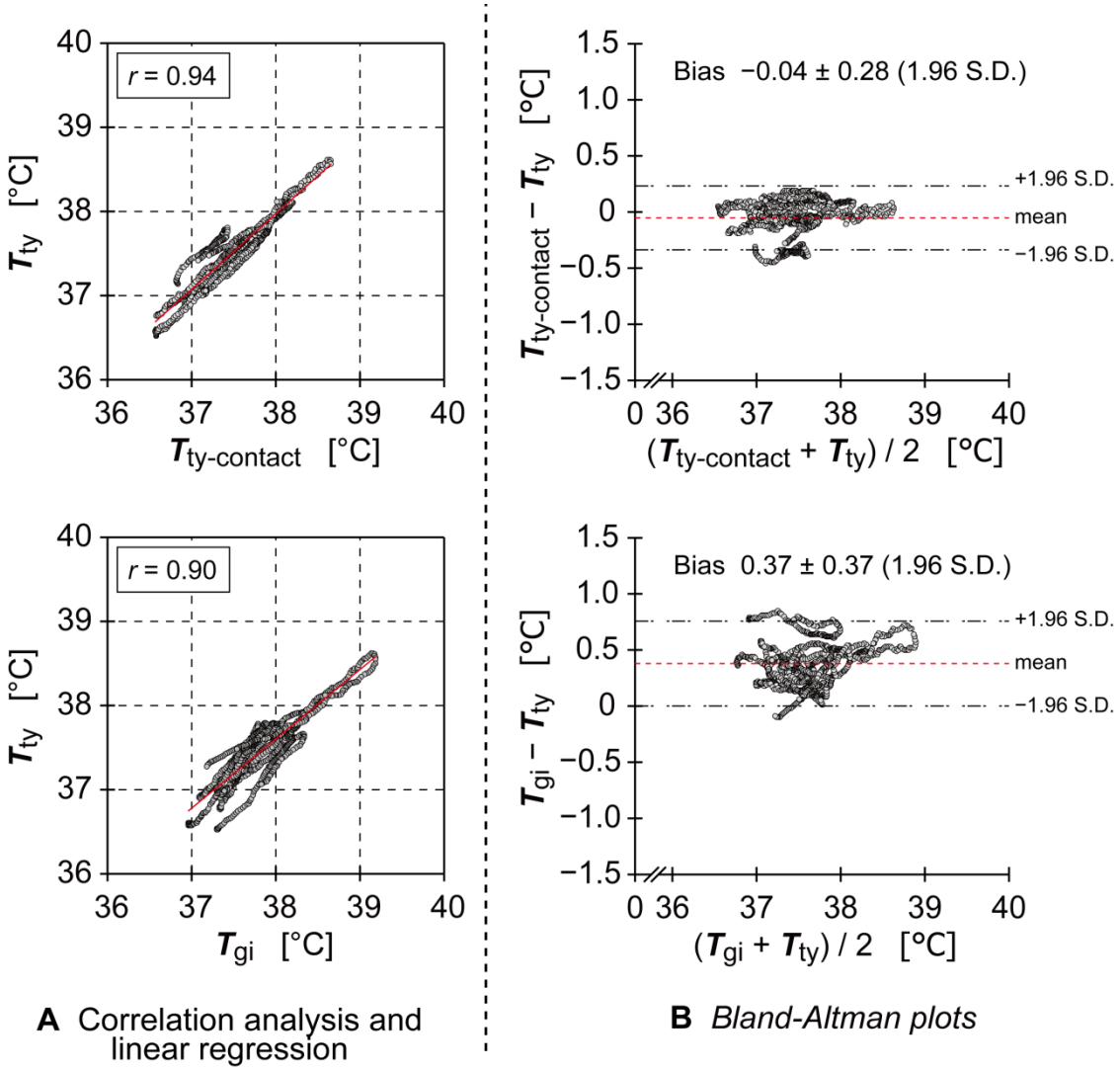

Figure 4.3 Statistical analysis results of comparative evaluation test during the cycle ergometer exercise. (A) The scatter plot for Pearson's correlation analysis and the linear regression between the contact tympanic temperature ($\boldsymbol{T}_{\text{ty-contact}}$) and the non-contact tympanic temperature measured by the present system ($\boldsymbol{T}_{\text{ty}}$), and that between the gastrointestinal temperature ($\boldsymbol{T}_{\text{gi}}$) and $\boldsymbol{T}_{\text{ty}}$, and (B) their *Bland-Altman* plots.

4.2. Most Suitable PPG Light Color for HR Monitor During Motion

4.2.1. Introduction

The reliability of HR derived from the PPG signals measured during normal daily life can be reduced by motion artifacts [32, 76]. Various techniques for the robust measurement of PPG signals during motion have been studied [32]. One approach, based on the optical characteristics of tissue, can be the choice of light wavelength [52-54]. The light sources used with PPG have been chosen at various wavelengths including the NIR (e.g., 810 or 940 nm), red, green, and blue [77]. NIR and red wavelengths are generally used in PPG research and for routine clinical applications [32]. But, among the possible light colors, green light PPG has been shown to have the least influence from motion artifacts when compared with the NIR light PPG [52-54].

Naturally, the influences of artifacts on the PPG signal are related to the wavelength of the light source [52-54, 78], simply because of the wavelength dependence of the light absorption (e.g., water, melanin, oxy- and deoxyhemoglobin) and therefore the penetration depth into the tissue [79-82]. Figure 4.4 shows the penetration depth for different colors of light in skin. Absorption of the longer wavelengths such as red and NIR is relatively low giving deeper tissue penetration [79, 80]. The PPG signal using red and NIR wavelengths arises mainly from the larger arterioles and possibly arteries in the deep dermis [52, 81, 82]. On the other hand, the shorter wavelengths of light, such as the green and blue, are strongly absorbed by melanin, and the penetration depth into the tissue is therefore relatively shallow [79-82]. According to Cui *et al.* [52], the influences of artifacts are larger in deeper site than in shallower site. Therefore, NIR and red light PPG is subject to artifacts, while the green and blue light PPG is relatively free from artifacts [52-54].

Despite the possible advantages of green light PPG, in terms of susceptibility to artifact little is known about the accuracy of HR measured by green light PPG during motion. Although Maeda *et al.* have examined the influence of artifacts on green light PPG signals as compared with NIR light PPG signal [53, 54], they did not compare with other wavelengths during motion. The purpose of the present study was to investigate the use of NIR, red, green, and blue light PPG to discover which of these is the most

suitable for measuring HR during normal daily life, where motion is likely to be a significant issue. I compared the HR measured by ECG as a reference with HR measured by NIR, red, green, and blue light PPG during a stationary state and with two kinds of intentional motion. The horizontal and vertical waving of the hand connected to the sensor was performed to produce these motion artifacts. In addition, I examined the signal-to-noise ratio (SNR) values produced by motion in the NIR, red, green, and blue light PPG [55].

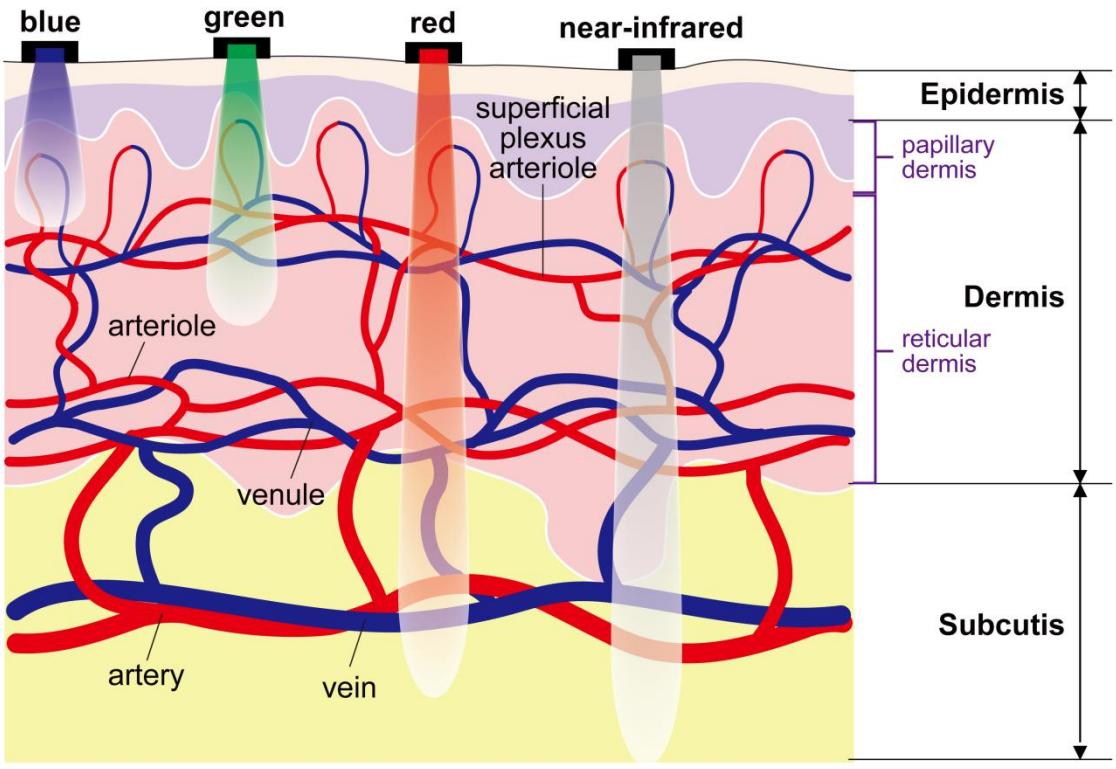

Figure 4.4 The skin structure and the penetration depth for different colors of light in tissue.

4.2.2. Experimental Method

4.2.2.1. Participants

Twelve healthy male participants, with a mean age of 22.8 ± 1.8 S.D. years, without known cardiovascular disorders participated in this study. All subjects agreed to take

part in this study voluntarily and signed an informed consent statement. The experimental design was approved by the ethics committee of the Kanazawa University.

4.2.2.2. Measurements

The PPG measurement device (sensor probe and amplifier) was built in the authors' laboratory [35]. The light sources and detectors used were as follow table 4.1

Table 4.1 The light sources and detectors of photoplethysmogpahy.

Sensor	Peak-wavelength [nm]	Bandwidth [nm]	Part number	Manufacturer
Near-infrared photo-sensor				
LED	810	35	SMC810	Epitex, Japan
PD	880	730~1100	BPW34FAS	OSRAM opto semiconductors, Germany
Red photo-sensor				
LED	645	22	LHT674	OSRAM opto semiconductors, Germany
PD	850	400~1100	BPW34S	OSRAM opto semiconductors, Germany
Green photo-sensor				
LED	530	33	LTT67C	OSRAM opto semiconductors, Germany
PD	540	430~610	TEMD5510FX01	Vishay semiconductors, USA
Blue photo-sensor				
LED	470	25	LBT67C	OSRAM opto semiconductors, Germany
PD	540	430~610	TEMD5510FX01	Vishay semiconductors, USA

Note. LED = light emitting diode; PD = PIN photodiode

The NIR, red, green and blue LED and its accompanying photodiode were placed side by side, thereby constituting the reflection mode PPG. Additionally, a NIR LED and its photodiode were placed on opposite sides, thereby constituting the transmission mode PPG. The distance of reflectance configuration sensors between LED and its accompanying photodiode are 5 mm (each pair of NIR and red) and 3 mm (each pair of green and blue), respectively. The each LED was operated in the pulsatile mode, receiving 250 us pulses at 16.6 ms intervals, to allow simultaneous measurement without interference between the each channel on the hand. The ECG was derived from limb leads (CM5) using disposable foam-pad electrodes connected to biopotential amplifier built in the authors' laboratory [83]. Peak point of the PPG signal and R point of the ECG signal were detected using a differentiating algorithm. HR was determined from peak-to-peak interval from the PPG and the R-R interval of the ECG, respectively. A 3-axis accelerometer (±6G, MMA7260Q, Freescale semiconductor, USA) was placed on the distal part of the finger to measure motion. The signals were recorded by a data acquisition card (NI USB-6218, National instruments, USA) with 1,024 Hz sampling rate, for storage and off-line analysis using LabVIEW (National instruments, Austin, USA).

4.2.2.3. Experimental Design

The experiments were performed in an air-conditioned laboratory (temperature: 26 °C, humidity: 62 %) in Kanazawa University. The participants sat on a chair, and then the disposable foam-pad electrodes, the accelerometer, and the three pairs of photo-sensors were attached. The photo-sensors were allocated sequentially in rotation between participants to either the index, middle and ring finger on the right hand so that each finger was used an equal number of times over the whole experiment.

The experiment was started with a 3 min rest period. Next, the participant underwent three conditions, each for 16sec: horizontal motion (HM), vertical motion (VM), and the stationary state as a baseline (BL). Each condition was separated by an 8 sec rest period, and the order of each condition was counter-balanced across participants. The set of three conditions was repeated three times. In the HM and VM periods, the participants waved their right hand connected to the sensor at a rate of 8 Hz paced by a computer metronome.

The whole experiment was repeated two times for each participant. Firstly, NIR light transmittance and reflectance configuration, and green light reflectance configuration were used as the three pairs of photo-sensors. And then, red, green and blue light reflectance configurations were used.

4.2.2.4. Data Analyses

All the stored data were equally subject to 30 Hz low pass digital filtering based upon the fast Fourier transform (FFT) algorithm. Beat-by-beat HR measured by the ECG was averaged for the each 16 sec condition.

Firstly, beat-by-beat HR measured by each PPG was averaged for each 16 sec HR condition. Next, Pearson's correlation analysis was performed between HR measured by ECG as a reference with that measured by the NIR, red, green, and blue light PPGs, respectively. Moreover, I conducted *Bland-Altman* analysis to evaluate their correspondence more closely [63].

Secondly, frequency spectral analysis for determined the SNR was performed using the pulse and acceleration wave by the 16,384 point FFT. Figure 4.5 shows the example of PPG and accelerometer waveforms power spectra for SNR calculation. FFT analysis was performed using BIMUTUS II (Kissei Comtec Co., Ltd., Japan) for Windows. The SNR value was calculated for each 16 sec condition. SNR is defined as the power ratio of pulse wave between the HR band with the motion artifact band, and it is expressed using the logarithmic decibel scale, as shown in equation.

$$\mathrm{SNR}\ [\mathrm{dB}] = 10\log_{10}\left(\frac{\boldsymbol{P}_{\text{heart rate band}}}{\boldsymbol{P}_{\text{motion artifact band}}}\right) \tag{4.1}$$

where $\boldsymbol{P}$ is the integrated power. The center frequency of the HR band and motion artifacts band are the mean frequency of HR measured by ECG and the peak frequency of motion measured by the accelerometer, respectively. Bandwidth of HR band and motion artifacts band are the mean HR frequency, while these bandwidths are the same (i.e., if mean HR = 60 bpm (1 Hz) and motion artifacts peak frequency = 8 Hz, then HR band is 0.5 ~ 1.5 Hz, motion artifacts band is 7.5 ~ 8.5 Hz). SNR values from the three repeated measurements were further averaged to produce single values for HM, VM,

and BL, respectively. Next, these values were compared statistically by means of the two-way analysis of variance (ANOVA), and then post-hoc comparison was performed by the Tukey's Honestly Significant Difference (Tukey HSD) test at the significance level of 5%.

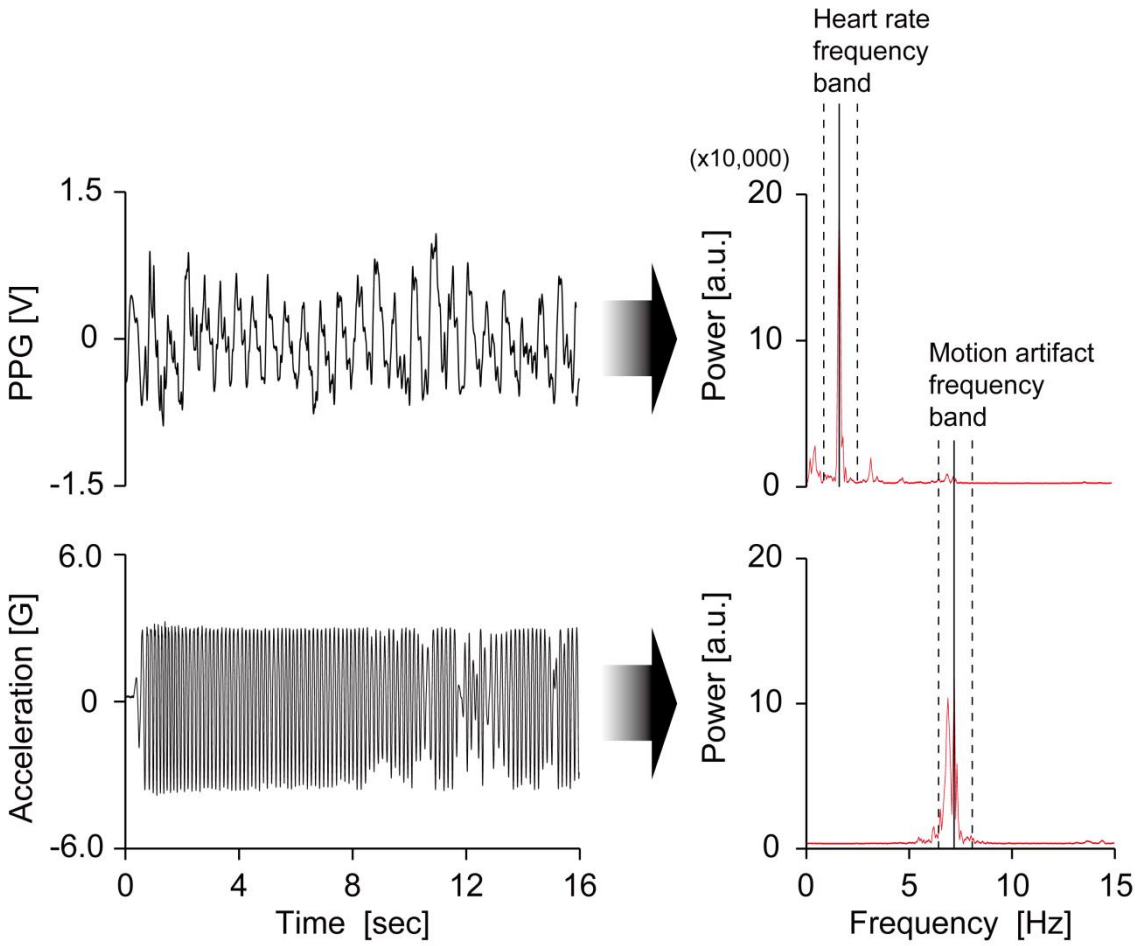

Figure 4.5 Example of photoplethysmography (PPG) and accelerometer waveforms power spectra for signal-to-noise ratio (SNR) calculation.

4.2.3. Results

The signal vector magnitude measured by the accelerometer periodically changed according to the motion of the right hand. A typical example of simultaneous recordings of the ECG, PPGt_NIR, PPGr_NIR, PPGr_green, and acceleration waveforms during

motion are shown in figure 4.6. Furthermore, those of the ECG, PPGr_red, PPGr_green, PPGr_blue, and acceleration waveforms are shown in figure 4.7.

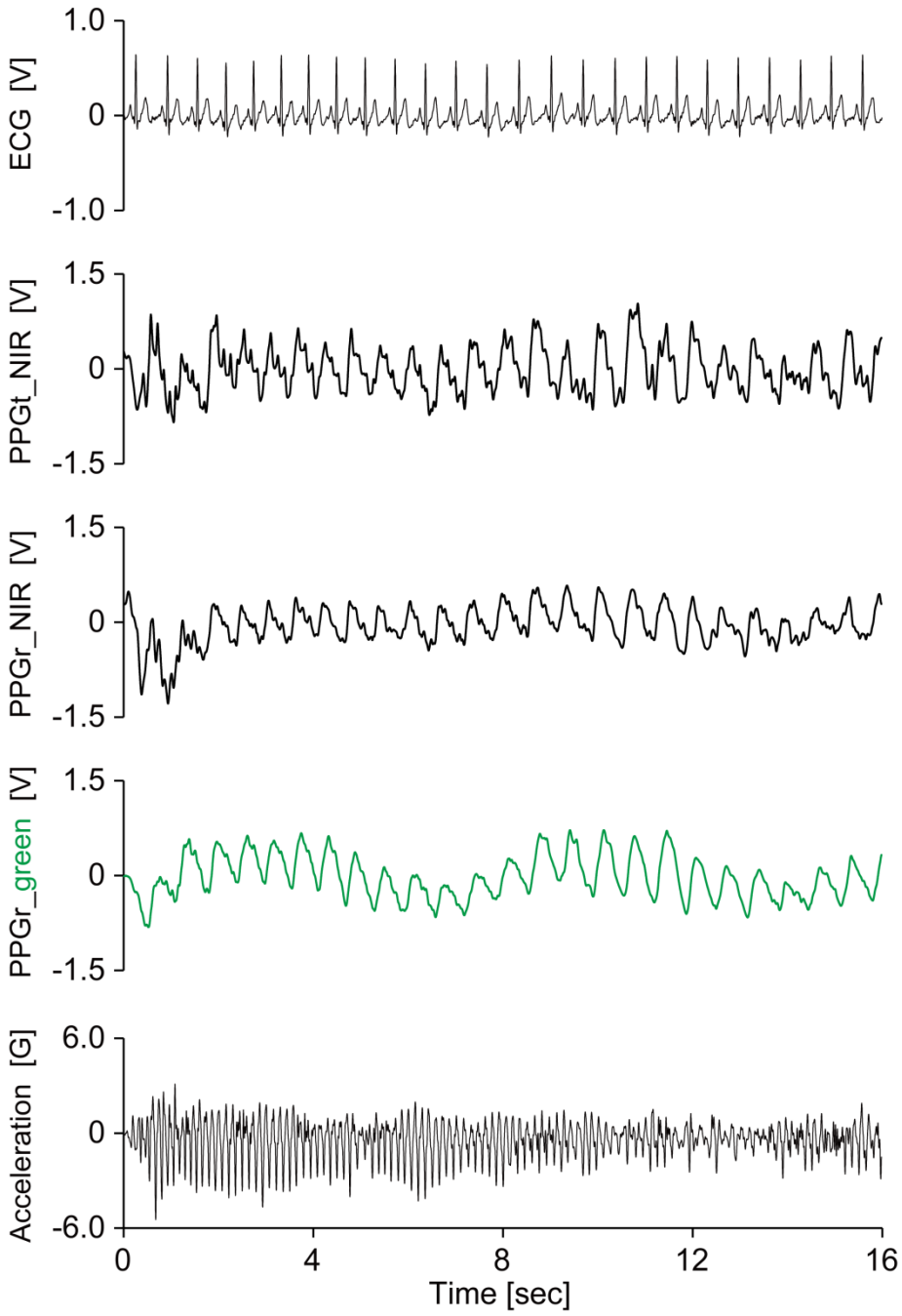

Figure 4.6 Typical trend-charts showing simultaneously recorded waveforms for near-infrared (NIR) and green light photoplethysmography (PPG). Waveforms for the electrocardiography (ECG), the near-infrared (NIR) light transmission and reflection mode PPG (PPGt_NIR and PPGr_NIR), green light reflection mode PPG (PPGr_green), and acceleration.

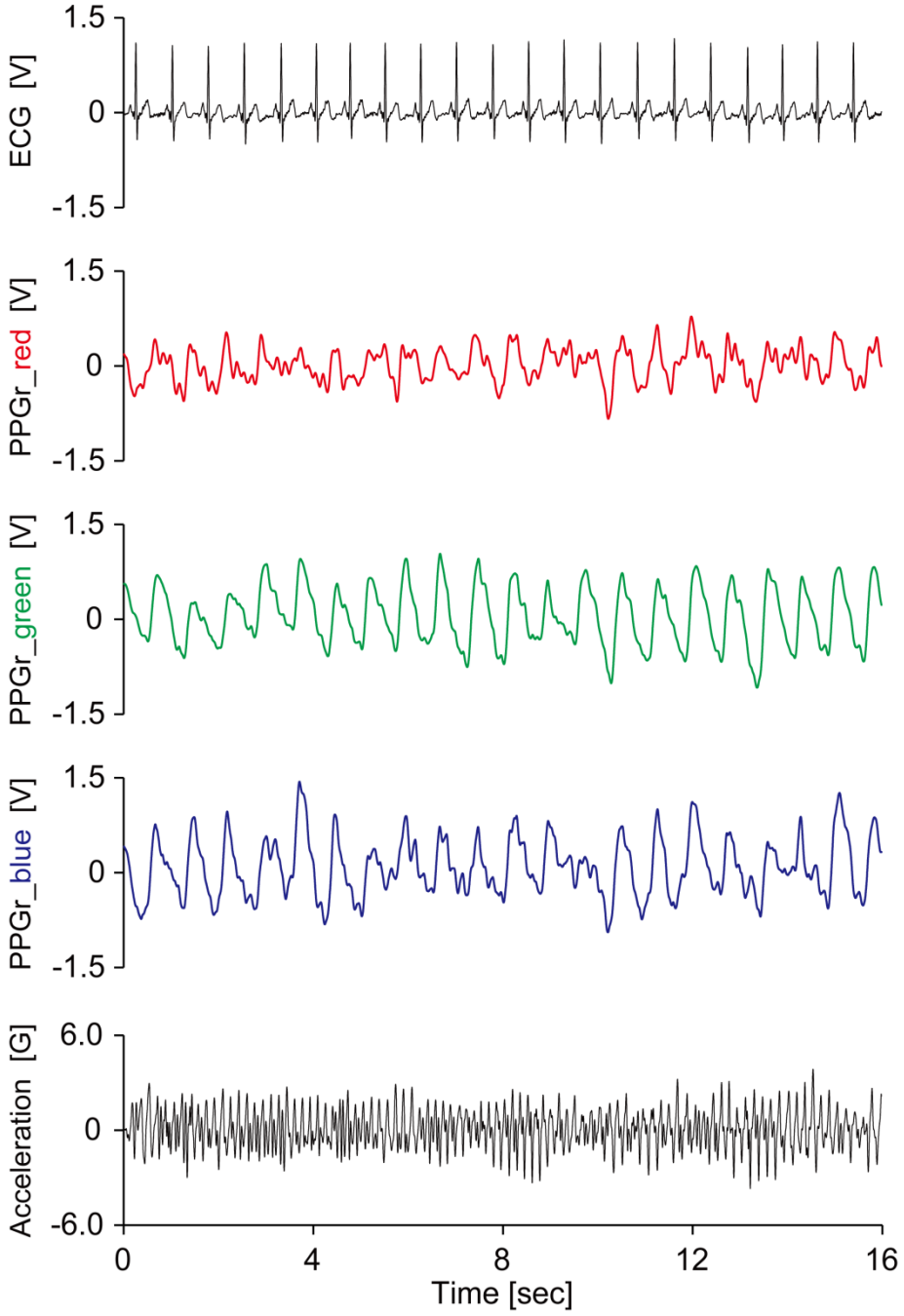

Figure 4.7 Typical trend-charts showing simultaneously recorded waveforms for red, green and blue light photoplethysmography (PPG). Waveforms for the electrocardiography (ECG), the red, green, and blue light reflection mode PPG (PPGr_red, PPGr_green, and PPGr_blue, respectively), and acceleration.

4.2.3.1. SNRs of NIR and green light PPG

Mean and standard error of the mean (S.E.M.) values of SNR are shown in figure 4.8 during the BL, HM, and VM. The two-way (3 PPG[PPGt_NIR, PPGr_NIR, PPGr_green] × 3 conditions [BL, HM, VM]) repeated measures ANOVA within all participants revealed that the 3 PPG, F (2,22) = 35.56, $p < 0.001$, and the 3 condition, F (2,22) = 44.65, $p < 0.001$, main effect were significant, as well as the PPG group × conditions interaction, F (4,44) = 6.52, $p < 0.001$.

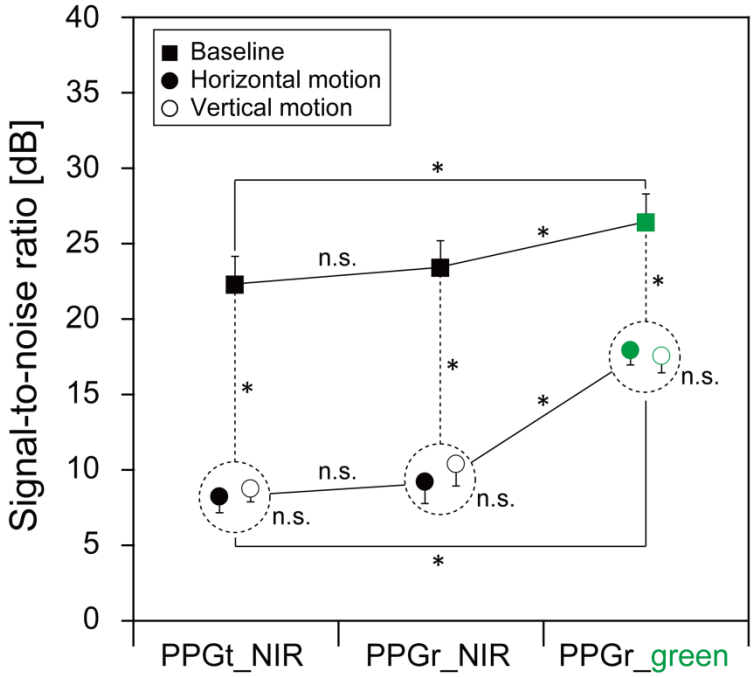

Figure 4.8 Mean of the signal-to-noise ratio (SNR) for near-infrared (NIR) and green light photoplethysmography (PPG). The NIR light transmission mode PPG (PPGt_NIR), NIR and green light reflection mode PPG (PPGr_NIR, and PPGr_green, respectively). Among the all condition (baseline, horizontal and vertical motion). Error bar is standard error of the mean (S.E.M.). *$p < 0.05$.

Firstly, significant differences among each PPG were found by Tukey HSD test: SNR values in the HM and VM were significantly higher the PPGr_green (17.97 ± 3.33 dB and 17.60 ± 3.88 dB) as compared to the PPGt_NIR (8.29 ± 3.71 dB and 8.82 ± 3.02 dB) and PPGr_NIR (9.28 ± 5.00 dB and 10.45 ± 5.07 dB), furthermore, SNR value in the BL was significantly higher the PPGr_green (26.43 ± 6.56 dB) as compared to the PPGt_NIR (22.30 ± 6.56 dB) and PPGr_NIR (23.42 ± 6.28 dB). But, SNR values in the

HM, VM, and BL showed no significant difference between the PPGt_NIR and PPGr_NIR. Secondly, significant differences among each condition were found by Tukey HSD test: SNR values of the PPGr_green, PPGt_NIR and PPGr_NIR were significantly lower in the HM and VM as compared to the BL. But, SNR values of the PPGr_green, PPGt_NIR and PPGr_NIR showed no significant difference between the HM with VM.

4.2.3.2. SNRs of red, green and blue light PPG

Mean and S.E.M. values of SNR are shown in figure 4.9 during the BL, HM, and VM respectively. The two-way (3 PPG [PPGr_red, PPGr_green, PPGr_blue] × 3 condition [BL, HM, VM]) repeated measures ANOVA within all participants revealed that the 3 PPG, F (2,22) = 37.72, $p < 0.001$, and the 3 condition, F (2,22) = 72.09, $p < 0.001$, main effect were significant, as well as the 3 PPG × 3 condition interaction, F (4,44) = 8.07, $p < 0.001$.

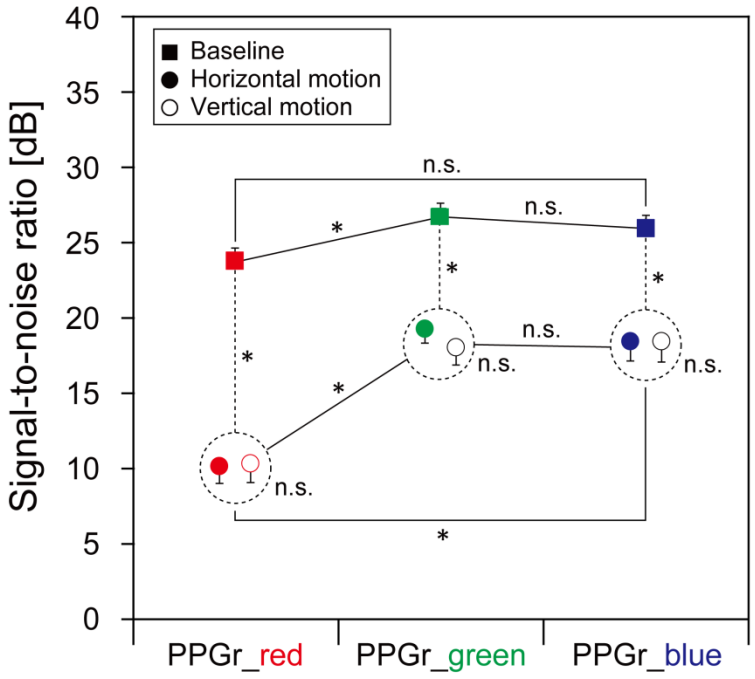

Figure 4.9 Mean of the signal-to-noise ratio (SNR) for red, green and blue light photoplethysmography (PPG). The red, green, and blue light reflection mode PPG (PPGr_red, PPGr_green, and PPGr_blue, respectively).Among the all condition (baseline, horizontal and vertical motion). Error bar is standard error of the mean (S.E.M.). *$p < 0.05$.

Significant differences among SNR value of 3 PPG were found by Tukey HSD test: SNR values in the HM and VM were significantly higher the PPGr_green (19.22 ± 3.30 dB and 17.99 ± 4.03 dB) and PPGr_blue (18.39 ± 4.55 dB and 18.39 ± 4.75 dB) as compared to the PPGr_red (10.12 ± 3.93 dB and 10.30 ± 4.38 dB), furthermore, SNR value in the BL was significantly higher the PPGr_green (26.63 ± 3.15 dB) as compared to the PPGr_red (23.72 ± 2.95 dB). But, SNR values in the BL showed no significant difference between PPGr_red andP PGr_blue (25.88 ± 2.98 dB). Also, SNR values in the HM and VM showed no significant difference between the PPG_green and PPG_blue. Secondly, significant differences among the 3 condition were found by Tukey HSD test: SNR values of the PPGr_red, PPGr_green and PPGr_blue were significantly lower in the HM and VM as compared to the BL. But, SNR values of the PPGr_red, PPGr_green and PPGr_blue showed no significant difference between the HM and VM.

4.2.3.3. Agreements of HR measured by NIR and green light PPG

Pearson's coefficient of correlation between HR measured by ECG (HR_ecg) as a reference and HR measured by the PPG using the NIR light transmittance configuration (HRt_NIR), NIR light reflectance configuration (HRr_NIR), and green light reflectance configuration (HRr_blue) are summarized in table 4.2 for the BL, HM, and VM, respectively.

Table 4.2 Pearson's coefficient of correlation between heart rate (HR) measured by electrocardiography (ECG) and HR measured by near-infrared (NIR) light transmission and reflection mode photoplethysmography (PPG), and green light reflection mode PPG.

	HR_ecg		
	Baseline	Horizontal motion	Vertical motion
HRt_NIR	0.999***	0.986***	0.997***
HRr_NIR	0.999***	0.973***	0.965***
HRr_green	0.999***	0.999***	0.999***

Note. HR_ecg = HR measured by ECG as a reference; HRt_NIR = HR measured by the NIR light transmission mode PPG; HRr_NIR = HR measured by the NIR light reflection mode PPG; HRr_green = HR measured by the green light reflection mode PPG. ***$P < 0.001$.

The three *Bland-Altman* plots between HR_ecg and HRt_NIR, HRr_NIR, and HRr_green are shown in figure 4.10 (A), 4.10 (B), and 4.10 (C), respectively. According to the *Bland-Altman* analysis, the mean differences (fixed biases) between HR_ecg with HRt_NIR, HRr_NIR, and HRr_green were +0.01 bpm, +0.23 bpm, −0.15 bpm, and limits of agreement were ±2.32 bpm, ±4.36 bpm, ±0.59 bpm, respectively.

4.2.3.4. Agreements of HR measured by red, green and blue light PPG

Pearson's coefficient of correlation between HR measured by ECG (HR_ecg) as a reference and HR measured by the reflection mode PPG using the red light (HRr_red), green light (HRr_green), and blue light (HRr_blue) are summarized in table 4.3 for the BL, HM, and VM, respectively.

Table 4.3 Pearson's coefficient of correlation between heart rate (HR) measured by electrocardiography (ECG) and HR measured by red, green, and blue light reflection mode photoplethysmography (PPG) [55].

	HR_ecg		
	Baseline	Horizontal motion	Vertical motion
HRr_red	0.999^{***}	0.967^{***}	0.995^{***}
HRr_green	0.999^{***}	0.999^{***}	0.999^{***}
HRr_blue	0.999^{***}	0.991^{***}	0.992^{***}

Note. HR_ecg = heart rate measured by ECG as a reference; HRr_red = HR measured by the red light reflection mode PPG; HRr_green = HR measured by the green light reflection mode PPG; HRr_blue = HR measured by the blue light reflection mode PPG. $^{***}P < 0.001$.

The three *Bland-Altman* plots between HR_ecg and HRr_red, HRr_green, and HRr_blue are shown in figure 4.11 (A), 4.11 (B), and 4.11 (C), respectively. According to the *Bland-Altman* analysis, the mean differences (fixed biases) between HR_ecg with HRr_red, HRr_green, and HRr_blue were −0.07 bpm, +0.18 bpm, +0.20 bpm, and limits of agreement were ±3.20 bpm, ±0.61 bpm, ±2.23 bpm, respectively.

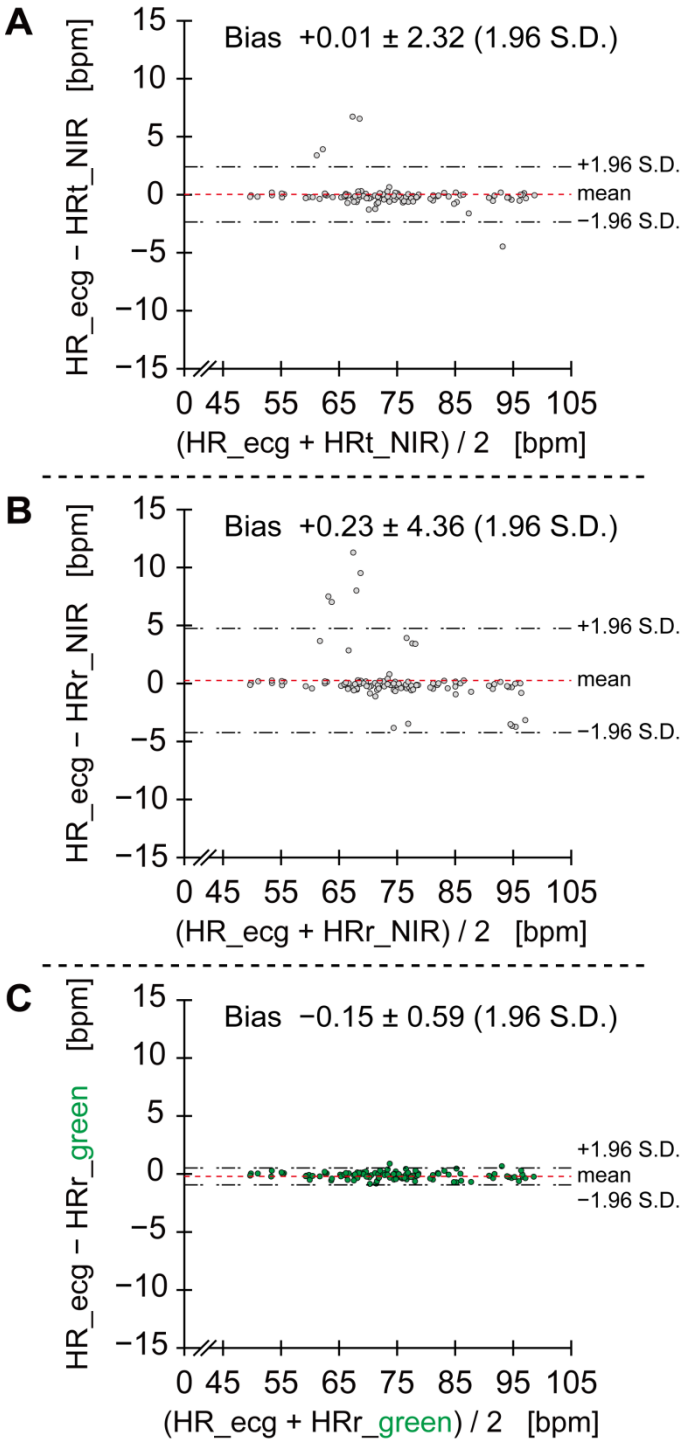

Figure 4.10 Three *Bland-Altman* plots between the heart rate (HR) derived from electrodardiograohy (ECG) as a reference and the HR derived from the NIR and green light photoplethysmography (PPG). (A) HR derived from ECG (HR_ecg) and HR derived from NIR light transmission mode PPG (HRt_NIR), (B) HR_ecg and HR derived from NIR light reflection mode PPG (HRr_NIR), and (C) HR_ecg and HR derived from green light reflection mode PPG (HRr_green), respectively. Among the all condition (baseline, horizontal and vertical motion).

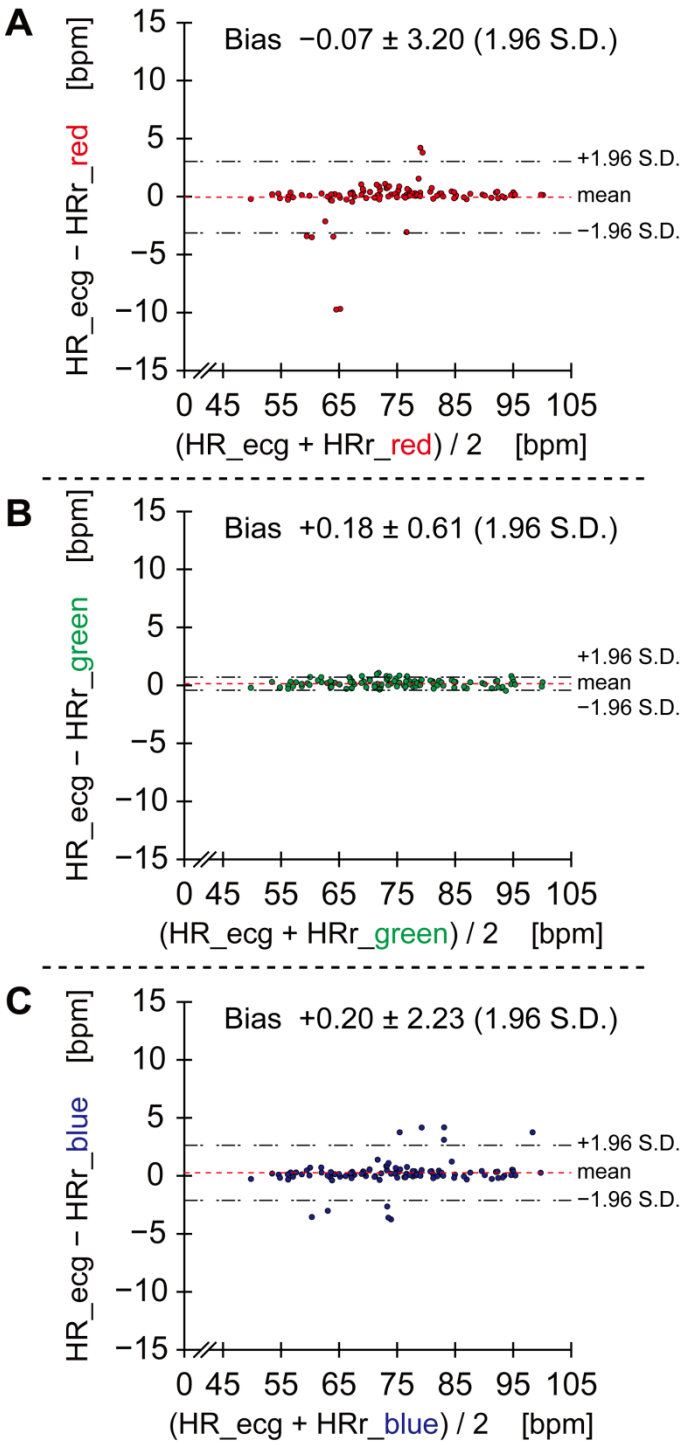

Figure 4.11 Three *Bland-Altman* plots between the heart rate (HR) derived from electrodardiography (ECG) as a reference and the HR derived from the red, green and blue light photoplethysmography (PPG) [55]. (A) HR derived from ECG (HR_ecg) and HR derived from red light reflection mode PPG (HRr_red), (B) HR_ecg and HR derived from green light reflection mode PPG (HRr_green), and (C) HR_ecg and HR derived from blue light reflection mode PPG (HRr_blue), respectively. Among the all condition (baseline, horizontal and vertical motion).

4.3. Modified Normalized Pulse Volume

4.3.1. Introduction

NPV derived from the photoplethysmograph, which is based on the Beer-Lambert-Bouguer law that describes the relationship between the intensity of incident light ($\boldsymbol{I}_o$) and transmitted light ($\boldsymbol{I}$), when the light passes through a non-scattering medium. If it is assumed that this law can be applied for transmission measurements in the fingertip, the relationship between the pulsatile change in the arterial blood volume, $\Delta \boldsymbol{V}_a$, and the intensity of the transmitted light could be derived. Within this context, the use of the transmission PPG obtained from a finger to derive the NPV has been analyzed theoretically with the application of the Beer-Lambert-Bouguer law [43]. It was shown that NPV could be derived simply by normalizing the magnitude of the ac component to the mean dc component, giving the following relationship:

$$\mathrm{NPV} = \Delta \boldsymbol{I}_{\mathrm{ac}} / \boldsymbol{I}_{\mathrm{dc}} \left(\propto \Delta V_a \right) \tag{4.2}$$

Equation (4.2) shows that the peak-to-trough magnitude of the ac component ($\Delta \boldsymbol{I}_{ac}$) is essentially corrected by the mean intensity of transmitted light, which is the mean dc component ($\boldsymbol{I}_{dc}$) photoplethysmographically detected from the finger. Thus, NPV is in direct proportion to the pulsatile component of the arterial blood volume, ΔV_a.

However, the validity of original NPV [43] must be questioned since it is based on the assumption that the light passes through a non-scattering medium. In fact, when light passes through biological tissues it is extensively scattered as well as absorbed. So, the modified Beer–Lambert–Bouguer law, which includes the influence of light-scattering, should be considered [56-58]. Furthermore, the tailored ear-piece is used the reflection mode PPG.

In the present experiment, I derived the modified NPV (mNPV) theory, which utilizes the modified Beer-Lambert-Bouguer law, to validate mathematical relationship in real biological tissues (light passes through absorptive and scattering). And, to validate the mNPV, I compared the mNPV derived from transmission mode PPG as a

reference with the mNPV derived from reflection mode PPG during the cold pressor test as physiological challenge [59].

4.3.2. Theory of Modified Normalized Pulse Volume

According to the modified Beer–Lambert–Bouguer law, the relation between $\boldsymbol{I}_o$ and $\boldsymbol{I}$, when the light passes through absorptive and scattering media, can be expressed as

$$-ln\left(\boldsymbol{I}/\boldsymbol{I}_o\right) = \varepsilon CkV + S \tag{4.3}$$

where ε is the molar absorptivity of the medium, C is the molar concentration of the medium. k is a volume correction factor, which is defined as the average of the differential path-length of light caused by scattering in the medium between light source and PD. If the light passes through a non-scattering medium then $k = 1$, whilst when there is scattering, $k > 1$. V is the volume of the medium where there is non-scattering (i.e. $k = 1$), and S is the attenuation due to scattering. Equation (4.3) can be rewritten as

$$-ln\left(\boldsymbol{I}/\boldsymbol{I}_o\right) = \varepsilon CV_c + S \tag{4.4}$$

where $\boldsymbol{V}_c$ is the corrected volume: $\boldsymbol{V}_c = k\boldsymbol{V}$.

I consider the fingertip being composed of three components: arterial and venous blood and ischemic tissue. If I assume that the modified Beer–Lambert–Bouguer law holds in the fingertip, the relation between $\boldsymbol{I}_o$ and $\boldsymbol{I}$ can be expressed by the following equation:

$$-l\,n\left(\boldsymbol{I}/\boldsymbol{I}_o\right) = \varepsilon_{\,a}\,C_a\,V_c + a\;\varepsilon\quad C_v\;V + c\;\varepsilon_v\quad C_t + V_{t\;+c\;t}\,S \tag{4.5}$$

Here ε_a, ε_v, and ε_t, are the absorptivity of the arterial blood, venous blood, and tissue, respectively. Similarly, C_a, C_v, and C_t, are the hematocrit (i.e. concentration of hemoglobin) of the arterial and venous blood, as well as the concentration of the tissue

absorbers, respectively. V_{ca}, V_{cv}, and V_{ct}, are the correction volume of the arterial blood, venous blood, and the ischemic tissue, respectively. S_{a+v+t} is the attenuation due to scattering under a normal circulatory state in which arterial and venous blood and bloodless-tissue all contribute to scatter.

Next, I consider the situation in which the finger is made to be ischemic, there then being only bloodless-tissue present. Now the relationship between $\boldsymbol{I}_o$ and the transmitted light intensity, $\boldsymbol{I}_t$, is given as:

$$-ln\left(\boldsymbol{I}_t/\boldsymbol{I}_o\right) = \varepsilon_t C_t V_{ct} + S_t \tag{4.6}$$

where S_t is the attenuation due to scattering by the bloodless-tissue under an ischemic circulatory state.

Subtracting equation (4.6) from equation (4.5), and using the exponential transform, yields the following equation:

$$\boldsymbol{I}/\boldsymbol{I}_t = e^{\left(-\varepsilon C V_c + S\right)} \tag{4.7}$$

where V_c is the corrected volume of the total blood, ε is the mean absorptivity of the total blood and S is the scattering attenuation of the total blood: $V_c = V_{ca} + V_{cv}$, $\varepsilon_a = (\varepsilon_a V_{ca} + \varepsilon_v V_{cv}) / V_c$, and $S = S_{a+v+t} - S_t$, respectively. C_a and C_v are considered to be constant and equal to the mean concentration of the total blood under a normal circulatory state [85], thus $C_a = C_v = C_t$.

The first derivative of $\boldsymbol{I}/\boldsymbol{I}_t$ with respect to V_c in equation (4.7) leads to:

$$d\left(\boldsymbol{I}/\boldsymbol{I}_t\right)/\, d\, V_c = -\varepsilon C\left(\boldsymbol{I}/\boldsymbol{I}_t\right) \tag{4.8}$$

and this subsequently leads to:

$$\Delta V_c = -\left(\varepsilon C\right)^{-1} \Delta \boldsymbol{I}/\boldsymbol{I} \tag{4.9}$$

Here, ΔV_c consists of the volume correction factor and the pulsatile components of the total blood volume: $\Delta V_c = k\Delta V$. Although the total blood volume consists of the mean and pulsatile components of the arterial blood volume, as well as of the venous blood volume, pulsation is only observed in arterial and arteriolar blood, so ΔV and the corresponding $\Delta \boldsymbol{I}$ may be rewritten as ΔV_a and $\Delta \boldsymbol{I}_{\mathrm{ac}}$, respectively. Correspondingly, $\boldsymbol{I}$ may be rewritten as $\boldsymbol{I}_{\mathrm{dc}}$.

$$\Delta V_a = -\left(k\varepsilon C\right)^{-1} \Delta \boldsymbol{I}_{\mathrm{ac}} / \boldsymbol{I}_{\mathrm{dc}} \tag{4.10}$$

The normalized pulse volume, NPV, being equal to the ratio of the ac and dc PPG components, $\Delta \boldsymbol{I}_{\mathrm{ac}}/\boldsymbol{I}_{\mathrm{dc}}$, is therefore simply derived from equation (4.10). It can be seen that NPV is related to the pulsatile component of the arterial blood volume, ΔV_a. Furthermore, there may be considered to be direct proportionality on the assumption that the mean absorptivity (ε), the hematocrit (C) and the volume correction factor (k) of the total blood are constant. Thus, from equation (4.10), I may state the modified NPV (mNPV):

$$\mathrm{mNPV} \propto \Delta \boldsymbol{I}_{\mathrm{ac}} / \boldsymbol{I}_{\mathrm{dc}} \propto \Delta V_a \tag{4.11}$$

This theoretical derivation, which utilizes the modified Beer–Lambert–Bouguer law, serves to validate the use of the mNPV mathematical relationship in real biological tissues where there are both absorptive and scattering processes. This provides more confidence in the use of the NPV index when the method is applied to reflection PPG, where multiple scattering events are key aspects of photon propagation.

It is noteworthy, however, that, regardless of the starting point, the final result as seen in equation (4.11) is the same as equation (4.2). Therefore, I have justified in using the term “NPV” instead of “mNPV”. Nevertheless, although the derivation described above confirms that there is no need to distinguish between the NPV using the transmission mode PPG (NPVt) and that using the reflection mode PPG (NPVr), for clarity in the present study I continue to specify NPVt and NPVr.

4.3.3. Experimental Method

4.3.3.1. Participants

Two groups of participants, ten young male participants (young group; age: 21.8 ± 1.0 S.D. years), and six middle-aged male participants (middle-aged group; age:48.8 ± 10.9 S.D. years), without known cardiovascular disorders participated in the present study. All participants were requested to refrain from drinking alcohol and carrying out exercise for at least 24 hours before the laboratory experiment, and from smoking, eating, and taking caffeinated beverages for least 2 hour before. All participants agreed to take part in this study voluntarily and signed an informed consent statement. The experimental design was approved by the ethics committee of the Kanazawa University.

4.3.3.2. Measurements

The PPG measurement device (probe and amplifier) was built in the authors' laboratory [35].

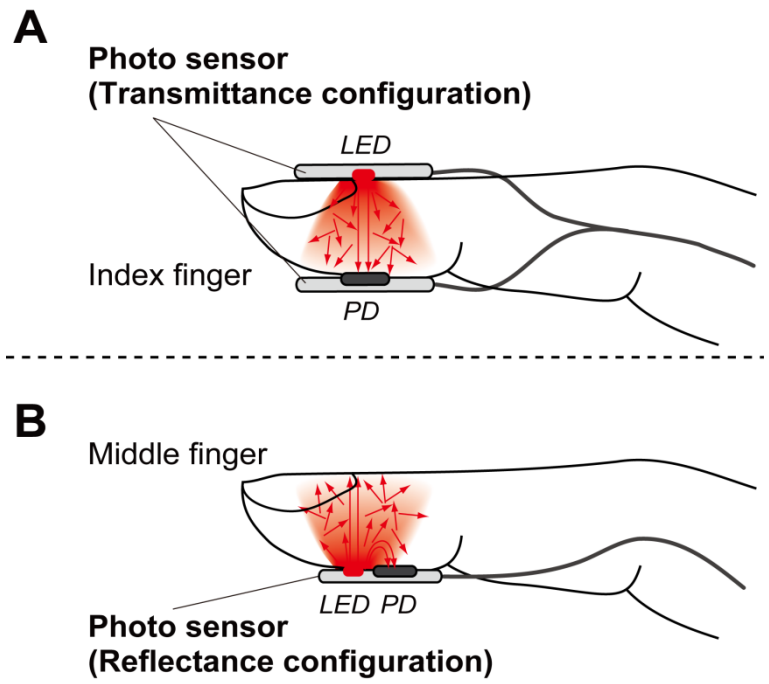

Figure 4.12 Attachment configurations of finger photo-sensors for measurement of normalized pulse volume (NPV). (A) Left-side hand index finger: the transmission type photo-sensor as a reference. (B) Left-side hand middle finger: the reflection type photo-sensor.

NIR LEDs (940 nm, VSMB1940X01, Vishay Semiconductors, USA) were used as light sources and PIN photodiodes (BPW34FS, sensitive area 7.0 mm^2, OSRAM opto semiconductors, Germany) as the detectors. Figure 4.12 shows the attachment configuration of photo-sensors for the measurement of NPV. ANIR LED and a photodiode were placed on opposite sides of the distal part of the index finger of the left hand, in the transmission mode PPG (see figure 4.12 panel A). The other NIR LED and photodiode of each pair being placed side by side of the distal part of the middle finger of the left hand, in the reflection mode PPG (see figure 4.12 panel B). The ac and dc photodiode outputs were amplified with gains of 150 and 1 respectively using a high precision OP-Amp. PPG was recorded by a data acquisition card (DAQ-6036, National Instruments Corp., Austin, USA) with an adapter (BNC-2111, National Instruments Corp., Austin, USA) at the 1 kHz sampling rate and a resolution of 16 bits, for storage and off-line analysis using LabVIEW (National Instruments Corp, Austin, USA) for Windows in a computer (Dell Latitude 5430).

4.3.3.3. Experimental Design

The experiments were performed in a quiet, auto air-conditioned laboratory (temperature: 26°C; humidity: 53%) in the Kanazawa University. At the start the participants sat on a chair to relax, and then the sensors were attached on the index and middle finger of the left hand. Each photo-sensor was fixed with the elastic adhesive bandage on the finger-tip. PPG was controlled by adjusting the intensity of the LED to achieve a better pulse (ac component) shape.

Participants were subjected to challenge: CPT (4°C) of the right hand up to the wrist to induce peripheral vasoconstriction [86-88]. The stages of the experiment were carried out in the following order while the participants sat quietly: (a) adaptation for 10 min; (b) baseline (BL) for 5 min; (c) the CPT for 90 s; (d) rest for 5 min.

4.3.3.4. Data Analyses

All the stored PPG data were equally subject to 30 Hz low pass digital filtering based upon the FFT algorithm. NPV was calculated from the PPG by dividing the peak-to-trough magnitude of ac component by the dc component. And then, logarithmic transformation was applied to NPV to normalize the distribution (*ln*NPV). *ln*NPV

values were averaged over 10 s, and these values further averaged to produce BL, first (CPT1; 0–30 s), second (CPT2; 30–60 s) and third (CPT3; 60–90 s) parts of four CPT values, respectively. These values were compared statistically by means of the one-way ANOVA, and then post-hoc comparison was performed by the Ryan's method.

Furthermore, *ln*NPV reactivities (Δ*ln*NPV) were calculated by subtracting the BL values from the CPT values (CPT1, CPT2 and CPT3). Then, Pearson's correlation analysis was performed between Δ*ln*NPV derived from the transmission mode finger PPG (Δ*ln*NPVt) as a reference and Δ*ln*NPV derived from the reflection mode finger PPG (Δ*ln*NPVr).

4.3.4. Results

4.3.4.1. *ln*NPV in young group

Mean and S.D. values of *ln*NPV derived from the transmission and reflection mode finger PPG (*ln*NPVt and *ln*NPVr, respectively) for the young group are summarized in table 4.4. The one-way ANOVA revealed the main effect of period: F (3,27) = 107.80, $p < 0.001$ for *ln*NPVt, and F (3,27) = 80.68, $p < 0.001$ for *ln*NPVr. Significant differences among each period were found by Ryan's method: BL > CPT1, CPT2 and CPT3, in both *ln*NPV.

Table 4.4 Mean (S.D.) values of *ln*NPV derived from finger photoplethysmography (PPG) using transmission and reflection type sensors in the 'young' group, during baseline and while performing the cold pressor test [59].

		Cold pressor test (CPT)		
	Baseline (5 min)	CPT1 (0 ~ 30 s)	CPT2 (30 ~ 60 s)	CPT3 (60 ~ 90 s)
*ln*NPVt [a.u.]	−3.20 (0.26)	-4.40^{***} (0.26)	-4.77^{***} (0.31)	-4.63^{***} (0.38)
*ln*NPVr [a.u.]	−6.20 (0.23)	-7.55^{***} (0.36)	-7.85^{***} (0.41)	-7.68^{***} (0.45)

Note. PPG = photoplethysmography; NPV = normalized pulse volume; *ln*NPV = logarithmically-transformed NPV; *ln*NPVt = *ln*NPV using the transmission mode PPG; *ln*NPVr = *ln*NPV using the reflection mode PPG; S.D.= standard derivation; a.u. = arbitrary unit.
The comparisons between 5 min mean during baseline and CPT mean for each 30 s block by Ryan's method.
$^{***}p< 0.001$, $^{**}p< 0.01$, $^{*}p< 0.05$.

4.3.4.2. *ln*NPV in middle-aged group

Mean and S.D. values of *ln*NPVt and *ln*NPVr for the middle-aged group are summarized in table 4.5. The one-way ANOVA revealed the main effect of period: F (3,15) = 49.38, $p < 0.001$ for *ln*NPVt, and F (3,15) = 50.85, $p < 0.001$ for *ln*NPVr. Significant differences among each period were found by Ryan's method: BL > CPT1, CPT2 and CPT3, in both *ln*NPV.

Table 4.5 Mean (S.D.) values of *ln*NPV derived from finger photoplethysmography (PPG) using transmission and reflection type sensors in the 'middle-aged' group, during baseline and while performing the cold pressor test [59].

		Cold pressor test (CPT)		
	Baseline (5 min)	CPT1 (0 ~ 30 s)	CPT2 (30 ~ 60 s)	CPT3 (60 ~ 90 s)
*ln*NPVt [a.u.]	−3.57 (0.27)	-4.64^{***} (0.28)	-4.58^{***} (0.23)	-4.30^{***} (0.35)
*ln*NPVr [a.u.]	−6.27 (0.23)	-7.45^{***} (0.13)	-7.29^{***} (0.20)	-7.02^{***} (0.27)

Note. PPG = photoplethysmography; NPV = normalized pulse volume; *ln*NPV = logarithmically-transformed NPV; *ln*NPVt = *ln*NPV using the transmission mode PPG; *ln*NPVr = *ln*NPV using the reflection mode PPG; S.D.= standard derivation; a.u. = arbitrary unit.
The comparisons between 5 min mean during baseline and CPT mean for each 30 s block by Ryan's method.
$^{***}p< 0.001$, $^{**}p< 0.01$, $^{*}p< 0.05$.

4.3.4.2. Agreement of *ln*NPV reactivities

During the CPT, strong relationships in both age groups are observed between Δ*ln*NPVt and Δ*ln*NPVr. Figure 4.13 shows the two scatter plots for the correlation and the linear regression during the CPT between Δ*ln*NPVt and Δ*ln*NPVr in the young group (see figure 4.13 panel A) and middle-aged (see figure 4.13 panel B) group, respectively.

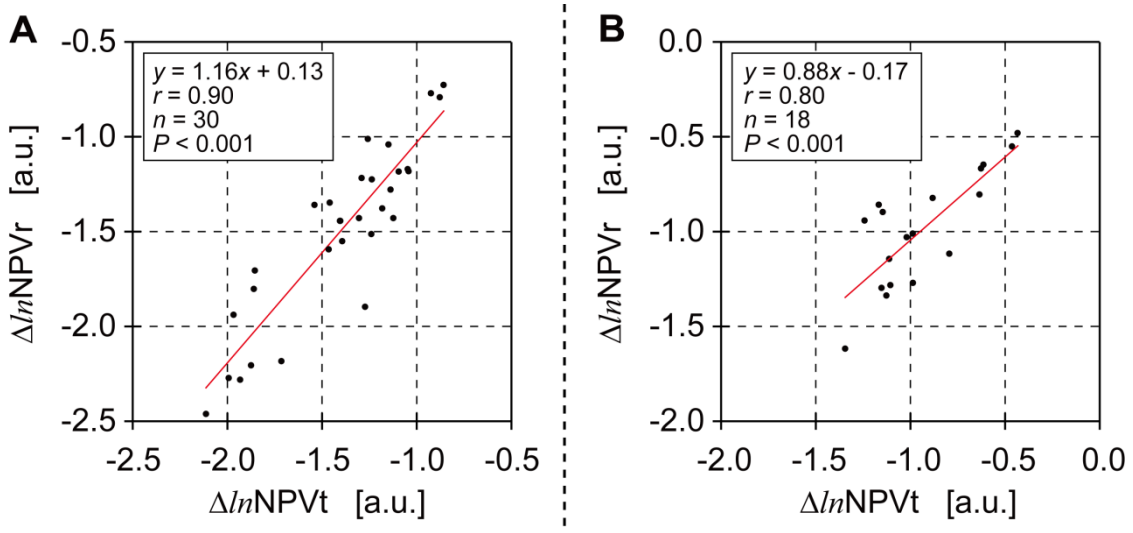

Figure 4.13 Two scatter plots of *ln*NPV reactivities derived from two different photoplethysmography (PPG) [59]. (A) In the 'young' group, Pearson's correlation analysis and the linear regression between Δ*ln*NPV from an index finger using transmission mode PPG (Δ*ln*NPVt) as a reference and Δ*ln*NPV from a middle finger using reflection mode PPG (Δ*ln*NPVr). (B) In the 'middle-aged' group, between Δ*ln*NPVt and Δ*ln*NPVr. During baseline and while performing cold pressor test, Δ*ln*NPV is the reactivities (the difference between baseline and test values) of *ln*NPV. Δ*ln*NPV is expressed in arbitrary units (a.u.).

4.4. Ear Normalized Pulse Volume

4.4.1. Introduction

Traditionally, the photoplethysmogram has been obtained from the fingertip with the light source and detector in the transmission configuration. This site is particularly useful for studying autonomic control since the arteriolar vessels here are known to be very sensitive to vasoconstrictor stimuli [88]. Other anatomical sites have also been used, in some cases, such as the toe and ear lobe, with transmission optodes and in other cases, including the forehead and esophagus, using the reflectance configuration [32, 39]. Of all of these possible sites, the different locations on and in the ear can have several advantages. The vessels of the deep auricular artery, which originates from either the maxillary or the superficial temporal artery, ascend through the bony wall of the ear-canal from the parotid gland under the ear-canal, with its branches providing a supply to the lining and periphery of the ear-canal [17-19]. Figure 4.14 shows the blood vessel of the ear-canal and auricle.

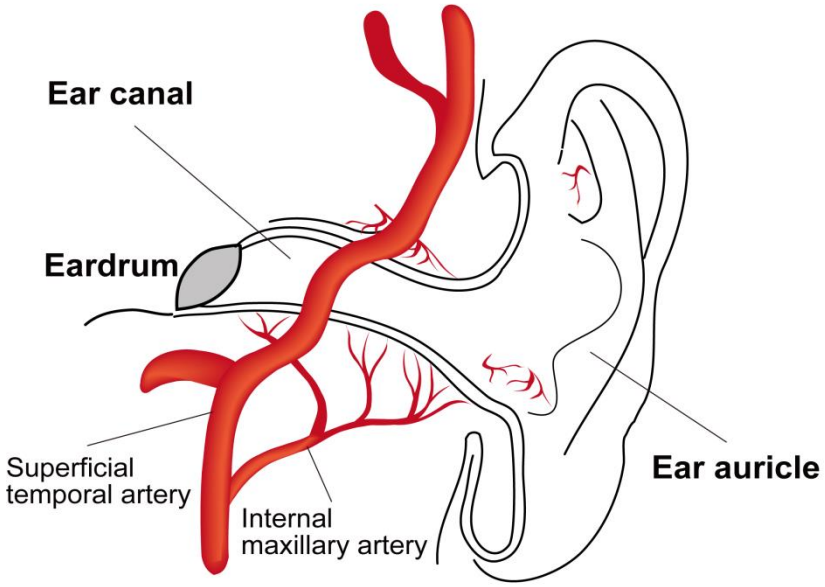

Figure 4.14 The blood vessel of the around ear-canal.

Thus, the photoplethysmogram can be obtained from there with the reflectance configuration. Furthermore there is relative freedom from motion artifacts produced, for example, during walking [40-42]. Therefore, the collection of PPG-derived

measurements from different regions of the ear could be well suited to the task of monitoring stress during normal daily life, especially through the use of the normalized pulse volume index, NPV.

Despite these potential advantages, the NPV derived from the ear has not yet been validated. Although Vogel *et al.* [41] have validated the measurement of heart rate using the PV recorded in the ear-canal (tragus), they did not validate NPV. Furthermore, the most suitable site around the ear-canal for the robust measurement of PPG signals using tailored ear-piece has not yet been examined. Therefore, the first purpose of the present experiment was to validate the ear NPV for evaluating thermal stress. The second purpose of the present experiment was to investigate the collection of PPG-derived measurements from different regions of the ear to discover where of these is the most suitable for measuring PPG using tailored ear-piece. I examined the PV (ac component) and $\boldsymbol{I}_{dc}$ (dc component) derived from the four different regions of the ear with the reflectance mode PPG. Also, I used NPV derived from an index finger with the transmission mode PPG configuration (NPVt_IF) as a reference. And then I compared the reference data with NPV values derived from the top and bottom of the ear-canal (NPVr_ECT and NPVr_ECB, respectively), as well as from the upper and lower parts of the ear-auricle (NPVr_EAU and NPVr_EAL, respectively), in all cases using the reflection mode PPG configuration. I used cold pressor test as physiological challenge.

4.4.2. Experimental Method

4.4.2.1. Participants

Two groups of participants, ten young male participants (young group; age: 21.8 ± 1.0 S.D. years), and six middle-aged male participants (middle-aged group; age: 48.8 ± 10.9 S.D. years), without known cardiovascular disorders participated in the present study. All participants were requested to refrain from drinking alcohol and carrying out exercise for at least 24 hours before the laboratory experiment, and from smoking, eating, and taking caffeinated beverages for least 2 hour before. All participants agreed to take part in this study voluntarily and signed an informed consent statement. The experimental design was approved by the ethics committee of the Kanazawa University.

4.4.2.2. Measurements

The PPG measurement device (probe and amplifier) was built in the authors' laboratory [35]. NIR LEDs (940 nm, VSMB1940X01, Vishay Semiconductors, USA) were used as light sources and PIN photodiodes (BPW34FS, sensitive area 7.0 mm^2, OSRAM opto semiconductors, Germany) as the detectors.

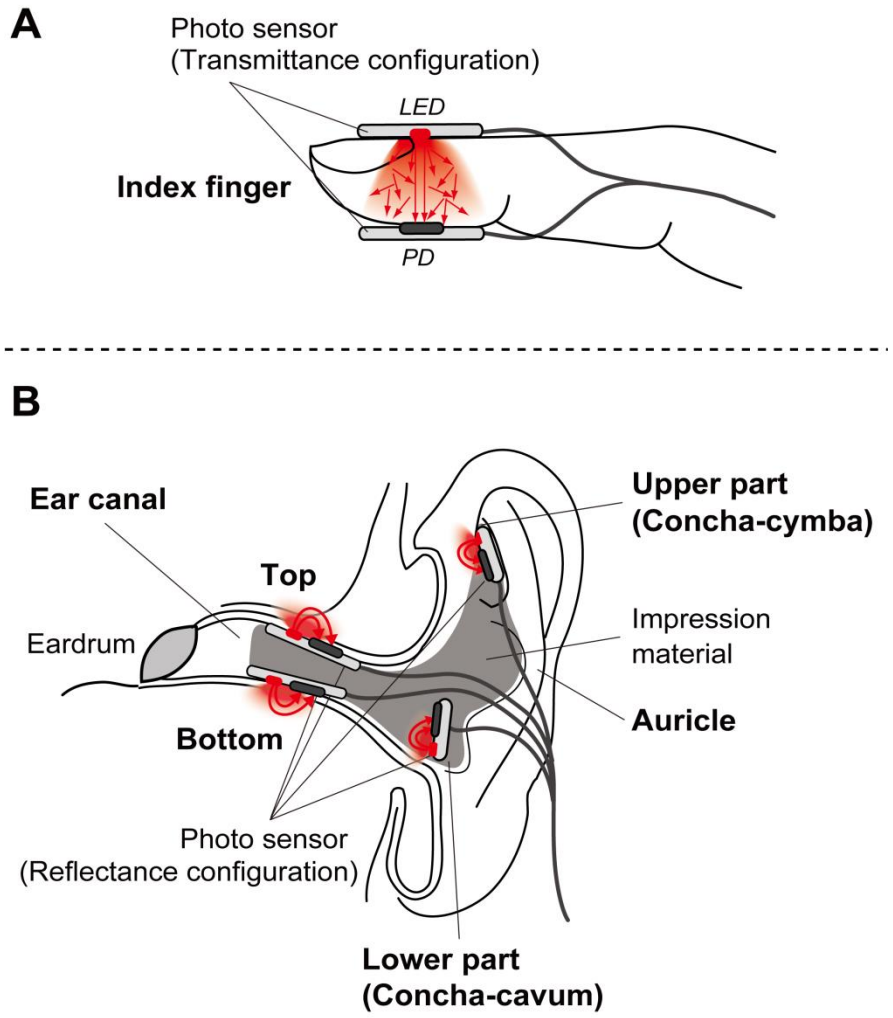

Figure 4.15 Attachment configurations of photo-sensors for the measurement of normalized pulse volume (NPV) [59]. (A) Left-side hand index finger: the transmission type photo-sensor as a reference. (B) Left-side ear: the top and bottom of the ear-canal, and the upper and lower part of the ear-auricle using the reflection type sensors.

Figure 4.15 shows the attachment configuration of photo-sensors for the measurement of NPV. A NIR LED and a photodiode were placed on opposite sides of the distal part of the index finger of the left hand, in the transmission mode PPG (see figure 4.15 panel A). For all other measurement sites the reflection mode PPG was used, with the LED and photodiode of each pair being placed side-by-side. The reflection sites were: at the top and bottom of the ear-canal (ECT and ECB, respectively); as well as the upper and lower part of the ear-auricle on the left ear (EAU and EAL, respectively) (see figure 4.15 panel B). The LEDs used in the ear were operated in the pulsatile mode, receiving 250 us pulses at 16.6 ms intervals, to allow simultaneous measurement without interference among the four channels in the ear. The ac and dc photodiode outputs were amplified with gains of 150 and 1 respectively using a high precision OP-Amp. PPG was recorded by a data acquisition card (DAQ-6036, National Instruments Corp., Austin, USA) with an adapter (BNC-2111, National Instruments Corp., Austin, USA) at the 1 kHz sampling rate and a resolution of 16 bits, for storage and off-line analysis using LabVIEW (National Instruments Corp, Austin, USA) for Windows in a computer (Dell Latitude 5430).

4.4.2.3. Experimental Design

The experiments were performed in a quiet, auto air-conditioned laboratory (temperature: 26 °C; humidity: 53%). At the start the participants sat on a chair to relax, and then the sensors were attached on the index finger of the left hand. The photo-sensor was fixed with the elastic adhesive bandage on the finger-tip. I carefully positioned the reflection type sensors in the ear-canal and the ear concha, and then secured them by infusing an impression material (detax addition, DETAX GmbH & Co. KG, Germany).

Participants were subjected to challenge: CPT (4°C) of the right hand up to the wrist to induce peripheral vasoconstriction [86-88]. The stages of the experiment were carried out in the following order while the participants sat quietly: (a) adaptation for 10 min; (b) baseline (BL) for 5 min; (c) the CPT for 90 s; (d) rest for 5 min.

4.4.2.4. Data Analyses

All the stored PPG data were equally subject to 30 Hz low pass digital filtering based upon the FFT algorithm. NPV was calculated from the PPG by dividing the peak-to-trough magnitude of ac component by the dc component. And then, logarithmic transformation was applied to PV, $\boldsymbol{I}_{dc}$, and NPV to normalize the distribution (*ln*PV, $ln\boldsymbol{I}_{dc}$, and lnNPV, respectively). *ln*PV, $ln\boldsymbol{I}_{dc}$, and *ln*NPV values were averaged over 10 s, and these values further averaged to produce BL, first (CPT1; 0–30 s), second (CPT2; 30–60 s) and third (CPT3; 60–90 s) parts of four CPT values, respectively. These values were compared statistically by means of the one-way ANOVA, and then post-hoc comparison was performed by the Ryan's method.

Furthermore, *ln*PV and *ln*NPV reactivities (Δ*ln*PV and Δ*ln*NPV) were calculated by subtracting the BL values from the CPT values. And then, Pearson's correlation analysis was performed between Δ*ln*NPVt_IF as a reference and Δ*ln*NPVr_ECT, Δ*ln*NPVr_ECB, Δ*ln*NPVr_EAU, and Δ*ln*NPVr_EAL, respectively, as well as, between Δ*ln*NPVt_IF as a reference and Δ*ln*PVr_ECT, Δ*ln*PVr_ECB, Δ*ln*PVr_EAU, and Δ*ln*PVr_EAL, respectively.

4.4.3. Results

4.4.3.1. *ln*PV, $ln\boldsymbol{I}_{dc}$, and *ln*NPV in young group

Mean and S.D. values of *ln*PV, $ln\boldsymbol{I}_{dc}$, and *ln*NPV for different anatomical positions, in the young group, are summarized in Table 4.6.

- *Index finger.* The one-way ANOVA revealed the main effect of period: F (3,27) = 75.44, $p < 0.001$ for *ln*PVt_IF; F (3,27) = 79.48, $p < 0.001$ for $ln\boldsymbol{I}_{dc}$t_IF; F (3,27) = 107.80, $p < 0.001$ for *ln*NPVt_IF. Furthermore, significant differences among each period were found by Ryan's method: BL > CPT1, CPT2, and CPT3 for *ln*PVt_IF and *ln*NPVt_IF; BL < CPT1, CPT2, and CPT3 for $ln\boldsymbol{I}_{dc}$t_IF.

Table 4.6 Mean (S.D.) values of *ln*PV, lnI_{dc}, and *ln*NPV for different anatomical positions in the 'young' group, during baseline and while performing the cold pressor test [59].

		Cold pressor test (CPT)		
	Baseline (5 min)	CPT1 (0 ~ 30 s)	CPT2 (30 ~ 60 s)	CPT3 (60 ~ 90 s)
Index finger				
*ln*PVt [mV]	2.57 (0.21)	1.69*** (0.26)	1.42*** (0.23)	1.55*** (0.27)
$ln\boldsymbol{I}_{dc}$t [mV]	5.38 (0.18)	5.66*** (0.19)	5.76*** (0.19)	5.76*** (0.20)
*ln*NPVt [a.u.]	−3.20 (0.26)	−4.40*** (0.26)	−4.77*** (0.31)	−4.63*** (0.38)
The top of the ear-canal				
*ln*PVr [mV]	0.54 (0.25)	0.36* (0.35)	0.36* (0.35)	0.41 (0.32)
$ln\boldsymbol{I}_{dc}$r [mV]	8.42 (0.08)	8.42* (0.08)	8.42* (0.08)	8.43* (0.08)
*ln*NPVr [a.u.]	−8.29 (0.26)	−8.40 (0.31)	−8.46 (0.38)	−8.42 (0.38)
The bottom of the ear-canal				
*ln*PVr [mV]	0.80 (0.35)	0.62** (0.37)	0.54*** (0.39)	0.57** (0.39)
$ln\boldsymbol{I}_{dc}$r [mV]	8.39 (0.08)	8.39 (0.08)	8.39 (0.08)	8.39 (0.09)
*ln*NPVr [a.u.]	−8.01 (0.37)	−8.18** (0.39)	−8.27*** (0.44)	−8.24** (0.44)
The upper part of the ear-auricle				
*ln*PVr [mV]	−0.25 (0.22)	−0.24 (0.21)	−0.24 (0.16)	−0.13 (0.17)
$ln\boldsymbol{I}_{dc}$r [mV]	8.39 (0.07)	8.39 (0.07)	8.39 (0.07)	8.39 (0.07)
*ln*NPVr [a.u.]	−9.06 (0.18)	−9.06 (0.21)	−9.05 (0.16)	−8.90 (0.26)
The lower part of the ear-auricle				
*ln*PVr [mV]	0.29 (0.35)	0.18 (0.29)	0.12* (0.26)	0.18 (0.23)
$ln\boldsymbol{I}_{dc}$r [mV]	8.40 (0.07)	8.40 (0.07)	8.40 (0.08)	8.40 (0.07)
*ln*NPVr [a.u.]	−8.52 (0.34)	−8.64 (0.29)	−8.70* (0.28)	−8.64 (0.22)

Note. PV = pulse volume (gain = 150); $\boldsymbol{I}_{dc}$ = intensity of PPG signal (gain = 1); PPG = photoplethysmography; NPV = normalized pulse volume; PVt, $\boldsymbol{I}_{dc}$t, NPVt = PV, $\boldsymbol{I}_{dc}$, and NPV using the transmission mode PPG, respectively; PVr, $\boldsymbol{I}_{dc}$r, NPVr = PV, $\boldsymbol{I}_{dc}$, and NPV using the reflection mode PPG, respectively; a.u. = arbitrary unit.
The comparisons between 5 min mean during baseline and CPT mean for each 30 s block by Ryan's method.
$^{***}p < 0.001$. $^{**}p < 0.01$. $^{*}p < 0.05$.

- *The top of the ear-canal.* The one-way ANOVA revealed the main effect of period: F (3,27) = 4.10, $p < 0.05$ for *ln*PVr_ECT; F (3,27) = 4.33, $p < 0.05$ for $ln\boldsymbol{I}_{dc}$r_ECT; F (3,27) = 4.33, $p < 0.1$ for *ln*NPVr_ECT. Significant differences among each period were found by Ryan's method: BL > CPT1 and CPT2 for *ln*PVr_ECT; BL < CPT1, CPT2 and CPT3 for $ln\boldsymbol{I}_{dc}$r_ECT.
- *The bottom of the ear-canal.* The one-way ANOVA revealed the main effect of period: F (3,27) = 8.43, $p < 0.001$ for *ln*PVr_ECB; F (3,27) = 8.44, $p < 0.001$ for *ln*NPVr_ECB. Significant differences among each period were found by Ryan's method: BL > CPT1, CPT2 and CPT3 for *ln*PVr_ECB and *ln*NPVr_ECB.
- *The upper part of the ear-auricle.* The one-way ANOVA revealed the main effect of period: F (3,27) = 3.05, $p < 0.05$ for *ln*PVr_EAU; F (3,27) = 2.79, $p < 0.1$ for $ln\boldsymbol{I}_{dc}$r_EAU; F (3,27) = 2.55, $p < 0.1$ for *ln*NPVr_EAU.
- *The lower part of the ear-auricle.* The one-way ANOVA revealed the main effect of period: F (3,27) = 3.47, $p < 0.05$ for *ln*PVr_EAL; F (3,27) = 3.61, $p < 0.05$ for *ln*NPVr_EAL. Significant differences among each period were found by Ryan's method: BL > CPT2 for *ln*PVr_EAL and *ln*NPVr_EAL.

4.4.3.2. *ln*PV, $ln\boldsymbol{I}_{dc}$, and *ln*NPV in middle-aged group

Mean and S.D. values of *ln*PV, $ln\boldsymbol{I}_{dc}$, and *ln*NPV for different anatomical positions, in middle-aged group, are summarized in Table 4.7.

- *Index finger.* The one-way ANOVA revealed the main effect of period: F (3,15) = 32.95, $p < 0.001$ for *ln*PVt_IF; F (3,15) = 76.24, $p < 0.001$ for $ln\boldsymbol{I}_{dc}$t_IF; F (3,15) = 50.85, $p < 0.001$ for *ln*NPVt_IF. Furthermore, significant differences among each period were found by Ryan's method: BL > CPT1, CPT2, and CPT3 for *ln*PVt_IF and *ln*NPVt_IF; BL < CPT1, CPT2, and CPT3 for $ln\boldsymbol{I}_{dc}$t_IF.
- *The bottom of the ear-canal.* The one-way ANOVA revealed the main effect of period: F (3,15) = 4.38, $p < 0.05$ for *ln*PVr_ECB; F (3,15) = 4.15, $p < 0.05$ for *ln*NPVr_ECB. Significant differences among each period were found by Ryan's method: BL > CPT2 for *ln*PVr_ECB and *ln*NPVr_ECB.

Table 4.7 Mean (S.D.) values of *ln*PV, lnI_{dc}, and *ln*NPV for different anatomical positions in the 'middle-aged' group, during baseline and while performing the cold pressor test [59].

		Cold pressor test (CPT)		
	Baseline (5 min)	CPT1 (0 ~ 30 s)	CPT2 (30 ~ 60 s)	CPT3 (60 ~ 90 s)
Index finger				
*ln*PVt [mV]	1.87 (0.47)	1.03^{***} (0.35)	1.15^{***} (0.32)	1.40^{***} (0.43)
$ln\boldsymbol{I}_{dc}$t [mV]	5.03 (0.35)	5.26^{***} (0.33)	5.32^{***} (0.30)	5.29^{***} (0.32)
*ln*NPVt [a.u.]	−3.57 (0.27)	-4.64^{***} (0.28)	-4.58^{***} (0.23)	-4.30^{***} (0.35)
The top of the ear-canal				
*ln*PVr [mV]	0.40 (0.23)	0.33 (0.22)	0.37 (0.15)	0.45 (0.16)
$ln\boldsymbol{I}_{dc}$r [mV]	8.46 (0.04)	8.46 (0.04)	8.46 (0.04)	8.46 (0.04)
*ln*NPVr [a.u.]	−8.48 (0.26)	−8.55 (0.25)	−8.51 (0.18)	−8.43 (0.20)
The bottom of the ear-canal				
*ln*PVr [mV]	0.66 (0.35)	0.51 (0.42)	0.46^{*} (0.43)	0.59 (0.40)
$ln\boldsymbol{I}_{dc}$r [mV]	8.46 (0.02)	8.46 (0.02)	8.46 (0.02)	8.46 (0.03)
*ln*NPVr [a.u.]	−8.21 (0.36)	−8.36 (0.44)	-8.42^{*} (0.45)	−8.29 (0.43)
The upper part of the ear-auricle				
*ln*PVr [mV]	0.08 (0.27)	0.14 (0.15)	0.30 (0.24)	0.30 (0.29)
$ln\boldsymbol{I}_{dc}$r [mV]	8.44 (0.03)	8.44 (0.03)	8.43 (0.04)	8.43 (0.03)
*ln*NPVr [a.u.]	−8.78 (0.26)	−8.73 (0.14)	−8.56 (0.27)	−8.56 (0.30)
The lower part of the ear-auricle				
*ln*PVr [mV]	0.11 (0.30)	0.05 (0.29)	0.08 (0.31)	0.20 (0.17)
$ln\boldsymbol{I}_{dc}$r [mV]	8.43 (0.02)	8.43 (0.02)	8.43 (0.02)	8.43 (0.02)
*ln*NPVr [a.u.]	−8.75 (0.34)	−8.81 (0.30)	−8.78 (0.30)	−8.66 (0.21)

Note. PV = pulse volume (gain = 150); $\boldsymbol{I}_{dc}$ = intensity of PPG signal (gain = 1); PPG = photoplethysmography; NPV = normalized pulse volume; PVt, $\boldsymbol{I}_{dc}$t, NPVt = PV, $\boldsymbol{I}_{dc}$, and NPV using the transmission mode PPG, respectively; PVr, $\boldsymbol{I}_{dc}$r, NPVr = PV, $\boldsymbol{I}_{dc}$, and NPV using the reflection mode PPG, respectively; a.u. = arbitrary unit.
The comparisons between 5 min mean during baseline and CPT mean for each 30 s block by Ryan's method.
$^{***}p < 0.001$. $^{**}p < 0.01$. $^{*}p < 0.05$.

4.4.3.3. Agreements of *ln*NPV reactivities derived from the ear

Pearson's correlation coefficient between Δ*ln*NPV at the index finger as a reference with Δ*ln*PV and Δ*ln*NPV from the middle finger and the different placements of the ear are presented in the young and middle-aged groups, respectively (table 4.8). In the young group, the significant relationships are observed between Δ*ln*NPVt_IF with Δ*ln*PVr_ECB, Δ*ln*NPVr_ECT, and Δ*ln*NPVr_ECB. In the middle-aged group, the significant relationships are observed between Δ*ln*NPVt_IF with Δ*ln*PVr_ECB, Δ*ln*PVr_EAL, Δ*ln*NPVr_ECB, and Δ*ln*NPVr_EAL. Figure 4.16 shows the two scatter plots for the correlation and the linear regression during the CPT between Δ*ln*NPVt_IF as a reference and Δ*ln*NPVr_ECB in the young group (see figure 4.16 panel A), and those in the middle-aged group (see figure 4.16 panel B), respectively.

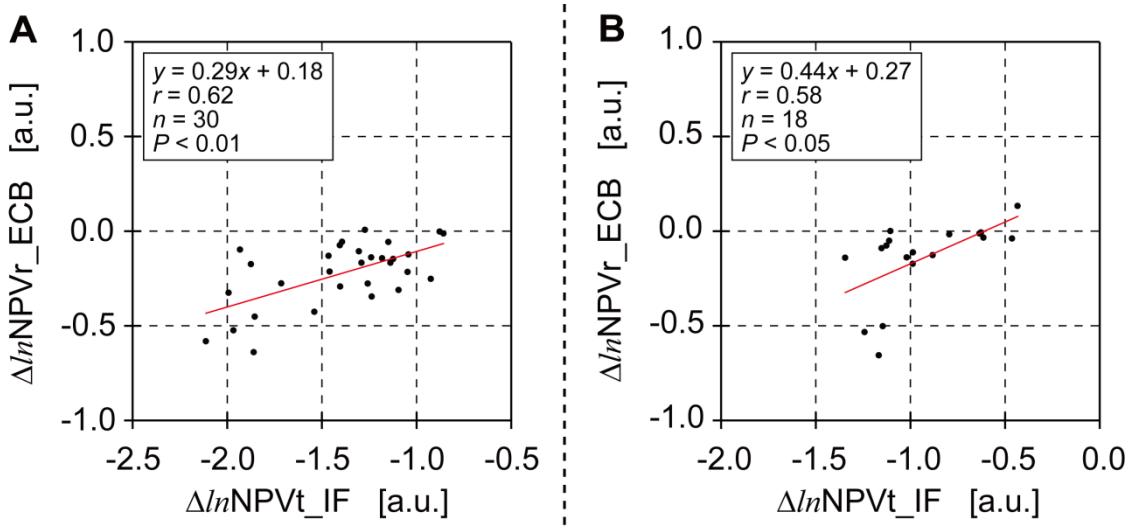

Figure 4.16 Two scatter plots of *ln*NPV reactivities derived from the index finger and the bottom of ear-canal [59]. (A) In the 'young'group, Pearson's correlation analysis and the linear regression between Δ*ln*NPV from an index finger using transmission mode PPG (Δ*ln*NPVt_IF) as a reference and Δ*ln*NPV from the bottom of the ear-canal using reflection mode PPG (Δ*ln*NPVr_ECB). (B) In the 'middle-aged' group, between ΔlnNPVt_IF and ΔlnNPVr_ECB. During baseline and while performing cold pressor test,Δ*ln*NPV is the reactivities (the difference between baseline and test values) of lnNPV.Δ*ln*NPVis expressed in arbitrary units (a.u.).

Table 4.8 Pearson's correlation coefficient of Δ*ln*NPV from an index finger using transmission mode photoplethysmography (PPG) as a reference with Δ*ln*PV and Δ*ln*NPV from the outer ear using reflection mode PPG in the 'young' and 'middle-aged' groups, respectively; during baseline and while performing cold pressor test [59].

	Δ*ln*NPVt_IF [a.u.]	
	in young group[a]	in middle-aged group[b]
The top of ear-canal		
Δ*ln*PVr [mV]	0.35	0.13
Δ*ln*NPVr [a.u.]	0.45*	0.14
The bottom of ear-canal		
Δ*ln*PVr [mV]	0.60**	0.59*
Δ*ln*NPVr [a.u.]	0.62**	0.58*
The upper part of the ear-auricle		
Δ*ln*PVr [mV]	0.18	−0.03
Δ*ln*NPVr [a.u.]	0.23	−0.04
The lower part of the ear-auricle		
Δ*ln*PVr [mV]	0.18	0.56*
Δ*ln*NPVr [a.u.]	0.18	0.56*

Note. PPG = photoplethysmography; Δ*ln*NPVt_IF = *ln*NPVt reactivities (the difference between baseline and test values) from an index finger using the transmission mode PPG as a reference; Δ*ln*PVr = *ln*PVr reactivities using the reflection mode PPG; Δ*ln*NPVr = *ln*NPVr reactivities using the reflection mode PPG; a.u. = arbitrary unit.
[a]$n = 30$. [b]$n = 18$.
$^{**}p < 0.01$. $^{*}p < 0.05$.

Chapter V.

Discussions

5.1. Reliability of Non-contact Tympanic Temperature Measurement

I have proposed and developed a new system for the continuous monitoring of tympanic temperature. The device allows tympanic temperature monitoring based on a new method, which I call “tailored ear-piece type tympanic thermometry”. The performance of the system was evaluated with in vivo tests to determine the accuracy in subjects immersed in a temperature-controlled water bath and during cycle ergometer exercise. The results clearly showed a strong correlation between the tympanic temperature measured with the newly developed system and both the contact tympanic temperature and the gastrointestinal temperature. Thus, I conclude that the tympanic temperature measure by the tailored ear-piece might be the reliable method to monitor of $\boldsymbol{T}_{\mathrm{c}}$ in heat condition and during exercise.

In order to compare tympanic temperature measured by the infrared-radiation-type sensor in the new device to direct tympanic and gastrointestinal temperatures, I made measurements in volunteers sitting in a temperature-controlled water bath, and exercising using the cycle ergometer. The results clearly showed, by linear regression analysis, a strong correlation between the infrared tympanic temperature and both the direct tympanic temperature and the gastrointestinal temperature. Further, the *Bland-*

Altman analysis demonstrated strong agreement between the pairs of measurements. Despite the apparent good performance of novel system there are certain potential problems. It could be argued that the infrared sensor might not detect the temperature of the tympanic membrane specifically. This is due to the crooked/curved nature of the ear canal in some participants, which means that the sensor can pick up 'noise' from the canal walls instead of only the tympanic membrane. In fact, this has previously been reported as a possible disadvantage of the infrared method [64-66]. However, the present experiment method employs a tailor-made ear-piece which effectively achieves a hermetically sealed condition. This could allow the ear canal wall temperature to equilibrate with the tympanic membrane. The strong correlation that I found between the infrared and direct tympanic temperature measurements suggests that this is a reasonable hypothesis.

The data presented in figure 4.2 and figure 4.3 requires further consideration. As can be seen, it appears that the temperature values from the contact and non-contact methods are almost the same at $\boldsymbol{T}_{\text{ty-contact}}$ values of 36.5 °C and 39.5 °C, with a larger difference at mid-range. This phenomenon is even more pronounced for the gastrointestinal temperature data (Figure 4.2 and figure 4.3). As previously reported [67], this phenomenon could be explained on the basis of a time-constant difference between the two different regions of the body, as well as by consideration of the two different measurement principles. In fact, this comparison test was done under non steady-state conditions and the influence of response time differences is therefore more apparent in the mid-range. If the mid-range differences shown in figure 4.2 and figure 4.3 are indeed due to these factors then the use of the measured tympanic temperature values will not adversely affect the usefulness of the new device under real measurement conditions. A further point is that the gastrointestinal temperature was found to be 0.27 °C and 0.37 °C higher than tympanic temperature. This tendency, which also exists for the rectal temperature, is consistent with the findings of previous studies [62, 67-70].

The ingestible telemetric pill method for obtaining the gastrointestinal temperature is another option for the practical measurement of $\boldsymbol{T}_{\text{c}}$, as used by us as a gold-standard reference in this study. In fact, recent studies dealing with heat stress problems in long distance runners have also reported the use of this method [71, 72]. However, recently-

published meta-analysis [69] and research [73] shows that the gastrointestinal temperature responds less rapidly than esophageal temperature at the start or cessation of exercise or to a change in exercise intensity, but more rapidly than rectal temperature. Additionally, it has been reported that the rectal temperature is affected by the physical activity of legs and arms [74]. This significant point is further emphasized in very recent work that has demonstrated very different rectal temperature measurements depending upon the depth of insertion of the rectal probe [75]. It is therefore apparent that there is no obvious ideal gold standard for $\boldsymbol{T}_c$ measurement in such complicated environmental situations and each potential anatomical site should be evaluated carefully within the context of the specific application for which it is intended.

5.2. Most Suitable PPG Light Color for HR Monitor During Motion

I compared the SNR of NIR, red, green, and blue light PPG waveforms and the agreement of HR measured by those, to discover which of these is the most suitable for measuring HR during normal daily life, where motion is likely to be a significant issue. The present experiment result clearly showed that, in terms of susceptibility to motion artifact, the green light PPG is better for the monitoring of HR during motion than the NIR, red and blue light PPG, and these results appear to be comparable to other studies for green light PPG [52-54]. In the first experiment for NIR and green light PPG, the limit of agreement between HR measured by green light PPG with HR measured by ECG as a reference was smaller than that between the HR measured by NIR light transmission and reflection mode PPG with HR measured by ECG (figure 4.10). Furthermore, the statistical analysis results showed that SNR value of the green light PPG in the baseline and horizontal and vertical motion was higher than both SNR value of the NIR light transmission and reflection mode PPG (figure 4.8) In addition, the second experiment for red, green and blue light PPG, the limit of agreement between the HR measured by green light PPG with HR measured by ECG as a reference was smaller than that between the HR measured by red and blue light PPG with HR measured by ECG (figure 4.11). Moreover, the statistical analysis results showed that SNRs of the

green light PPG produced by the HM and VM conditions were higher than those of the red light PPG (figure 4.9). Taken together, these findings suggest that the green light PPG appears to be the most suitable method for the monitoring of HR during normal daily life.

In contrast to the HR measured by green light PPG, the HR measured by NIR, red and blue light PPG gave poorer results. These results could be explained by the penetration depth of light into the tissue, but the reasons for these results probably differ from each other. The NIR and red light has a deep penetration depth into the tissue [79, 80]. The NIR and red light PPG reflects the volume change in the blood vessel in the dermis and subcutis. The subcutis consists of loose connective tissue (include blood vessel) and fat [84]. So, the NIR and red light PPG signal was quite sensitive to motion artifacts. That is, the poor results of HR measured by red light PPG could be caused by the large influence of motion artifact on the pulse wave itself. On the other hand, the SNR of blue light PPG were comparable to the SNR of green light PPG (figure 4. 9), while the limit of agreement between the HR measured by blue light PPG and HR measured by ECG was larger than that between HR measured by green light PPG and HR measured by ECG (figure 4.11). The green and blue light has a shallow penetration depth into the tissue [79, 80]. The green and blue light PPG reflects the volume change in blood vessel in the dermis, mainly. The ground substance of dermis is a semisolid matrix that allows dermal structures some movement [84]. So, the green and blue light PPG is relatively free from artifacts. Nevertheless, the poor results of HR measured by blue light PPG could be caused by the different shape of the pulse wave. The shape of the pulse wave depends upon the properties of the blood vessels [32]. The blue light PPG reflects the volume change in small blood vessel in the skin surface due to the relatively shallow penetration depth of blue light into the tissue [79, 80].

In this study, I have measured only the PPG at the finger-tip during waving motion. However, there are several body sites which pulses can easily be detected, examples including the ear, forehead, limb, and toe [32, 39]. Furthermore, the waving motion used in laboratory experimentation does not necessarily reflect normal daily life situations [76]. Therefore, further studies are needed to examine green light PPG at other sites during normal daily life.

5.3. Modified Normalized Pulse Volume

I have used the transmission mode PPG as well as the reflection mode PPG when measuring NPV. The transmission and reflection modes of PPG have been studied by others [89, 90], who reported that the pulsatile and non-pulsatile changes in intensity of light were found to be very similar whether measured by transmitted or reflected light. In this study although the each absolute value of *ln*NPV is different due to the volume correction factor (*k*), CPT produced strong statistical relationships between transmission PPG measurements in the index finger, Δ*ln*NPVt as a reference, and reflection measurements in the middle finger, Δ*ln*NPVr (figure 4.13). Taken together, these results support the view that the transmission mode PPG and the reflection mode PPG are indeed the comparable method to derive changes in NPV values.

In addition to these main results, there are other points related to NPV to consider. Firstly, I have performed the CPT in the right hand up to the wrist to induce peripheral vasoconstriction. As a result, *ln*NPVt and *ln*NPVr were significantly decreased from BL to CPT (table 4.4 and table 4.5). In fact, the CPT has been frequently used to induce peripheral vasoconstriction [86-88]. Therefore, these results suggest that the CPT successfully produced peripheral vasoconstriction.

Secondly, in the present experiment subjects were required to remain still with the effect that their central blood oxygen levels were assumed to be approximately constant and so the absorptivity (ε) could also be assumed to be essentially constant. This consideration is necessary when using the 940nm wavelength light source. However, the peripheral oxygen levels can be changed in various circumstances, especially normal daily life and it would therefore be preferable to use an isobestic wavelength, such as 805nm [36], to avoid this problem.

In this study, I have only used the cold pressor test as physiological challenge. To evaluate NPV, however, there are several tasks that may initiate peripheral vasoconstriction, examples including mental arithmetic, mirror tracing, and social speech [43, 87, 91]. Therefore, further laboratory studies using other kinds of stressors are needed to examine modified NPV more fully.

5.4. Ear Normalized Pulse Volume

NPV has been reported as being a more valid measure for the assessment of α-adrenergically mediated peripheral vascular tone [43]. Whilst the finger has traditionally been used as the most appropriate anatomical site for measuring the PPG, other sites are clearly possible [32, 39], and the ear could be advantageous in certain situations. The vessels of the deep auricular artery pass between the tragus and eardrum, with its branches providing a supply to the skin of the cartilaginous ear-canal [17-19]. As compared with measurements in the finger or the limbs PPG recorded from the ear can be relatively free from motion artifacts [41]. Thus, the collection of PPG-derived measurements from the ear could be well suited to the task of monitoring stress during normal daily life, for example through the use of the NPV index [43]. However, the NPV derived from the ear has not yet been validated and this was the purpose of the work described herein. In order to attempt to validate the NPV derived from PPG measurements at different sites in the ear, I have compared *ln*PV, $ln\boldsymbol{I}_{dc}$, and *ln*NPV with reference data derived from transmission PPG measurements in an index finger during cold pressor tests, CPT, as physiological challenges. Specifically I have compared the reference NPV values with the reflection PPG measurements, *ln*PVr and *ln*NPVr at different locations of the ear.

I have calculated NPV by dividing PV by the so-called dc component of the PPG. Naturally, if the dc component is essentially constant, NPV values will be directly proportional to the PV and the calculation of NPV is seemingly unnecessary. However, PV itself is affected by several instrumental and anatomical factors, including amplifier gain and skin color, and the normalization process to derive NPV minimises the adverse influence of these factors. In the present study, I kept these variables constant, so the correlation coefficient of ΔlnNPVt_IF versus ΔlnNPVr_ECB was comparable to that of ΔlnNPVt_IF versus ΔlnPVr_ECB (table 4.8) during the CPT. However, not all measurements can be conducted under such controlled conditions, especially if the system is to be used during normal daily life. Therefore, NPV derived at the ear could be more suited to the task of monitoring stress than PV.

The present experiment results show that, among the ear sites considered, the NPV

values derived from reflection PPG measurements at the bottom of the ear-canal (NPVr_ECB) have the closest relationships with the reference data. This is judged, firstly, by the significant decreases that are observed in *ln*NPVr_ECB from the baseline values to the values obtained during the CPT (table 4.6 and table 4.7). These decreases of *ln*NPVr_ECB indicate vasoconstriction by sympathetic activity during the exposure to the stressful stimuli [43, 45]. Secondly, good relationships were observed during the CPT between Δ*ln*NPVt_IF as the reference with Δ*ln*NPVr_ECB, (figure 4.16). These relationships could be explained by the reported location of the origin of the deep auricular artery on the lining of the ear-canal. The vessels of the deep auricular arteries ascend through the bony wall of the ear-canal from the parotid gland under the ear-canal, with branches providing a supply to the lining of the ear-canal [17-19]. That is, the change of the blood volume at the bottom of the ear-canal is larger than the change of the blood volume at the different placements of the ear. Taken together, these findings suggest that NPVr_ECB could be used as an alternative to NPVt_IF for evaluating physiological and psychological stress.

The results for NPV values derived from measurements at the top of the ear-canal (NPVr_ECT), were somewhat inferior to those from the bottom of the ear-canal, NPVr_ECB. Although *ln*NPVr_ECT fell from baseline to CPT (table 4.6 and table 4.7), the decreases were smaller than those of *ln*NPVr_ECB. These findings indicate that the sensitivity of NPVr_ECT during CPT was lower than that of NPVr_ECB. Furthermore, during the CPT, the correlation of Δ*ln*NPVt_IF versus Δ*ln*NPVr_ECT was lower than Δ*ln*NPVt_IF versus Δ*ln*NPVr_ECB as demonstrated by both analyses (table 4.8). Therefore, although NPVr_ECT could also be used as an alternative to NPVt_IF, if NPVr_ECB is available then it is to be preferred.

In contrast to the NPV data derived from the top and bottom of the ear-canal, NPVr_ECT and NPVr_ECB respectively, the indices derived from measurements at the upper (EAU) and lower (EAL) regions of the ear-auricle, gave poorer results. Although the CPT induced changes in the NPV index the magnitudes of these changes were much less pronounced than those seen with the ear-canal measurements. Falls in both NPV indices measured at the lower ear-auricle were produced by the CPT, but these were much smaller than those obtained in the ear-canal (table 4.6 and table 4.7). For upper ear-auricle measurements, during the CPT *ln*NPVr_EAU did not fall significantly from

the baseline values (table 4.6 and table 4.7). Furthermore, the CPT did not produce any statistically significant relationships between Δ*ln*NPVt_IF and either Δ*ln*NPVr_EAU, or Δ*ln*NPVr_EAL (table 4.8). These results suggest that the NPV indies derived from PPG measurements at the upper and lower regions of the ear-auricle, NPVr_EAU and NPVr_EAL respectively, are not ideally suited to the task of monitoring stress. This could imply that the supply to the auricle regions is more sparse; there is perhaps an insufficient arterial supply to allow the measurement of NPV from those regions [17-19].

It is of significance that the results show that the pattern of the autonomic vascular control in the ear appears to be more complex than that in the finger. In general, autonomic control processes in the peripheral vasculature appears to mitigate the changes induced by stimuli [12, 46, 92, 93]. For example, the PV and total blood volume in the finger decreased during an exposure to stressful stimuli [43, 45]. In the present study, the decreases seen in the *ln*PV and $ln\boldsymbol{I}_{dc}$ indices derived from the finger during the CPT could be comparable to those findings. On the other hand, the *ln*PV in the ear-canal was found to fall during the CPT, while the $ln\boldsymbol{I}_{dc}$ in the ear-canal was maintained nearly constant during the CPT, although a significant change of $ln\boldsymbol{I}_{dc}$ at the top of the ear-canal was observed (table 4.6 and table 4.7). The nearly constant $ln\boldsymbol{I}_{dc}$ observed in the ear could be explained by the notion that the blood flow in the head and neck circulation is maintained relatively constant by cerebral auto-regulation [94]. So, the pattern of the autonomic vascular control in the ear-canal might be a mixture of the maintenance of total blood volume and vasoconstriction induced by exposure to stressful stimuli.

In addition to these main results, there are other points related to ear NPV to consider. Firstly, regardless of age group, the same tendencies in the results were observed; not only the significant decrease in *ln*NPVr_ECB from the baseline values to the values obtained during the CPT (table 4.6 and table 4.7), but also the significant relationship during the CPT between Δ*ln*NPVt_IF as the reference and Δ*ln*NPVr_ECB are observed (table 4.8), though the reactivities of each *ln*NPV during CPT in the middle-aged group is marginally smaller than those in the young group. These results mean that the pattern of the autonomic vascular control is very similar regardless of age. These findings provide more confidence in the NPVr_ECB as an alternative to NPVt_IF for evaluating physiological and psychological stress.

In this study, I have not yet shown that the ear NPV measurement performed with the methodology can actually be applied to the investigation of stresses experienced in normal daily life. This is because the stressful tasks used in laboratory experimentation do not necessarily reflect daily life situations, for example during working and sporting activities [95, 96]. Therefore, further studies are needed to examine ear NPV under normal daily life situations.

Chapter VI.

Conclusion and Limitations

6.1. Summary

In the present study, I have proposed the development of novel ear-type physiological variables monitoring system for healthcare in normal daily life, which I call "*ear-type smart monitor*". This novel system includes the two main applications: 1) the "*tailored ear-piece*" to measure of various physiological variables; and 2) the "*smartphone*" to monitor and data analyzing. This system was designed for the simultaneous and continuous monitoring of $\boldsymbol{T}_{\mathrm{c}}$, HR and NPV in the ear.

However, before the full-fledged development of prototype system, there have been four questions about methods of the physiological variable measurement; 1) the reliability of the novel tympanic temperature measurement method using the tailored ear-piece and an infrared-radiation-sensor for continuous monitoring; 2) the most suitable light color of PPG for measuring HR during normal daily life, where motion is likely to be a significant issue; 3) the validity of mNPV based on the modified Beer-Lambert-Bouguer law, which includes the influence of light-scattering and absorption in real biological tissues. (the mathematical relationship in real biological tissues, mNPV theory; the reflection mode PPG-derived mNPV reactivity to physiological challenge); and 4) the validity of NPV derived from ear, and the most suitable location around ear

for measuring PPG using tailored ear-piece. Therefore, I have performed four experiments, respectively, to develop the "*ear-type smart monitor*".

As the result;

1) The developed novel tympanic thermometry using the tailored ear-piece could be used to the reliable $\boldsymbol{T}_c$ monitor in a heat stress condition and during the cycle ergometer exercise [29-31].
2) The green (530 nm) light PPG was more suitable for monitoring of HR during motion than NIR (810 nm), red (645 nm) and blue (470 nm) light PPG [55].
3) Theoretically, regardless of the starting point, the final result in mNPV equation (include light-scattering and absorption) was the same as original NPV equation (assumed non-scattering in the tissue). Experimentally, the reflection mode PPG and the transmission mode PPG were indeed the comparable method to derive NPV values [59].
4) The NPV derived from the bottom of the ear-canal with reflection mode PPG was found to be a valid measure when compared with reference measurements made in an index finger under cold pressor tests to produce peripheral vasoconstriction [59].

In conclusion, these results suggest that the proposed "*ear-type smart monitor*" could allow the continuous monitoring of the $\boldsymbol{T}_c$ and NPV. Furthermore, if the green light PPG is used in the tailored ear-piece to measure of pulsation, the HR measured by this system during motion might be more reliable.

6.2. Limitations

This study was the basic experiment about the method of measuring $\boldsymbol{T}_c$, HR and NPV in the ear, and there were several possible limitations. Firstly, despite four basic experiments, there still remain several questions for physiological index measurement. It is the validity of NPV derived from the bottom of ear-canal using green light reflection mode PPG. The collection (PV, $\boldsymbol{I}_{dc}$ and NPV) of green light PPG-derived measurements from ear has not yet been examined (In the second experiment, the green

light PPG signals were measured at the fingers). Moreover, the reliability of HR derived from ear-canal using green light PPG in normal daily life, where motion is likely to be a significant issue, has not yet been examined. Therefore, further studies are needed to examine the HR and NPV derived from green light ear PPG under various situations as the field studies [31, 95, 96].

Secondly, in the experiments related to ear-measurement (tympanic temperature and ear NPV), I used the impression material as to fix the sensor in the inner ear. The prototype of tailored ear-piece with built-in sensors has not yet been developed. Furthermore, the simultaneous monitoring of $\boldsymbol{T}_c$, HR and NPV in the ear has not yet been examined. Therefore, further studies should be necessary to develop the tailored ear-piece prototype. Additionally, the reliability test of prototype is essential, and final studies are needed to examine the simultaneous monitoring of $\boldsymbol{T}_c$, HR and NPV with the smartphone application development such as *iPhysioMeter* [48].

Reference

[1] McMichael A. J., Woodruff R. E., and Hales S., "Climate change and human health: present and future risks," *Lancet,* vol. 367, no. 9513, pp. 859-69, 2006, doi:10.1016/S0140-6736(06)68079-3.

[2] Haines A., Kovats R. S., Campbell-Lendrum D., and Corvalan C., "Climate change and human health: impacts, vulnerability and public health," *Public Health,* vol. 120, no. 7, pp. 585-96, 2006, doi:10.1016/j.puhe.2006.01.002.

[3] Basu R. and Samet J. M., "Relation between elevated ambient temperature and mortality: a review of the epidemiologic evidence," *Epidemiol. Rev.,* vol. 24, no. 2, pp. 190-202, 2002, doi:10.1093/epirev/mxf007.

[4] Smoyer K. E., "A comparative analysis of heat waves and associated mortality in St. Louis, Missouri-1980 and 1995," *Int. J. Biometeorol.,* vol. 42, no. 1, pp. 44-50, 1998, doi:10.1007/s004840050082.

[5] Bouchama A. and Knochel J. P., "Heat stroke," *N. Eng. J. Med.,* vol. 346, no. 25, pp. 1978-88, 2002, doi:10.1056/NEJMra011089.

[6] Yamakoshi K., "In the spotlight: bioInstrumentation," *IEEE Rev. Biomed. Eng.,* vol. 6, pp. 9-12, 2013, doi:10.1109/RBME.2012.2227703.

[7] Yamakoshi T., Matsumura K., Rolfe P., Hanaki S., Ikarashi A., Lee J., and Yamakoshi K., "Potential for health screening using long-term cardiovascular parameters measured by finger volume-oscillometry: pilot comparative evaluation in regular and sleep-deprived activities," *IEEE J. Biomed. Heal. Inform.,* vol. 18, no. 1, pp. 28-35, 2014, doi:10.1109/JBHI.2013.2274460

[8] Yamakoshi T., Matsumura K., Hanaki S., Ikarashi A., Rolfe P., Lee J., Yamakoshi Y., Hirose H., and Yamakoshi K., "Development of a novel system based on the simultaneous measurement of physiological variables for safer driving and general daily healthcare," *Tran. Jpn. Soc. Med. Biol. Eng.,* vol. 50, no. 2, pp. 227-36, 2012.

[9] Yamakoshi K., "In the spotlight: bioInstrumentation," *IEEE Rev. Biomed. Eng.*, vol. 3, pp. 3-6, 2010, doi:10.1109/RBME.2010.2089616.

[10] Nakagawara M. and Yamakoshi K., "A portable instrument for non-invasive monitoring of beat-by-beat cardiovascular haemodynamic parameters based on the volume-compensation and electrical-admittance method," *Med. Biol. Eng. Comput.*, vol. 38, no. 1, pp. 17-25, 2000, doi:10.1007/BF02344683.

[11] Togawa T., "Home health care and telecare," in *Sensors applications, sensors in medicine and health care* vol. 3, Oberg P. A., Togawa T., and Spelman F. A., Eds., Germany: Wiley, 2006, pp. 381-404.

[12] Palatini P., Casiglia E., Gasowski J., Gluszek J., Jankowski P., Narkiewicz K., Saladini F., Stolarz-Skrzypek K., Tikhonoff V., Van Bortel L., Wojciechowska W., and Kawecka-Jaszcz K., "Arterial stiffness, central hemodynamics, and cardiovascular risk in hypertension," *Vasc. Health. Risk. Manag.*, vol. 7, pp. 725-39, 2011, doi:10.2147/VHRM.S25270.

[13] Rhee S., Yang B. H., and Asada H. H., "Artifact-resistant power-efficient design of finger-ring plethysmographic sensors," *IEEE Trans. Biomed. Eng.*, vol. 48, no. 7, pp. 795-805, 2001, doi:10.1109/10.930904.

[14] Lee J., Lee W. J., and Kim K. H., "A study on a portable health monitoring system with wristband using photoplethysmograph and skin temperature " *INFORMATION*, vol. 15, no. 8, pp. 3621-36, 2012.

[15] Poh M. Z., Swenson N. C., and Picard R. W., "A wearable sensor for unobtrusive, long-term assessment of electrodermal activity," *IEEE Trans. Biomed. Eng.*, vol. 57, no. 5, pp. 1243-52, 2010, doi:10.1109/tbme.2009.2038487.

[16] Poh M. Z., Swenson N. C., and Picard R. W., "Motion-tolerant magnetic earring sensor and wireless earpiece for wearable photoplethysmography," *IEEE Trans. Inform. Technol. Biomed.*, vol. 14, no. 3, pp. 786-94, 2010, doi:10.1109/titb.2010.2042607.

[17] Gray H. and Lewis W. H., *Anatomy of the human body*, 20th ed. Philadelphia and New York: Lea & Febiger, 1918.

[18] Alvord L. S. and Farmer B. L., "Anatomy and orientation of the human external ear," *J. Am. Acad. Audiol.*, vol. 8, no. 6, pp. 383-90, 1997.

[19] Lucente F. E., "Anatomy, histology, and physiology," in *The external ear*, Lucente F. E., Lawson W., and Novick N. L., Eds., Philadelphia: Saunders, 1995, pp. 1-17.

[20] Lim C. L., Byrne C., and Lee J. K. W., "Human thermoregulation and measurement of body temperature in exercise and clinical settings," *Ann. Acad. Med. Singap.*, vol. 37, no. 4, pp. 347-53, 2008.

[21] Robinson J. L., Seal R. F., Spady D. W., and Joffres M. R., "Comparison of esophageal, rectal, axillary, bladder, tympanic, and pulmonary artery temperatures in children," *J. Pediatr.*, vol. 133, no. 4, pp. 553-6, 1998, doi:10.1016/S0022-3476(98)70067-8.

[22] Shiraki K., Konda N., and Sagawa S., "Esophageal and tympanic temperature responses to core blood temperature changes during hyperthermia," *J. Appl. Physiol.*, vol. 61, no. 1, pp. 98-102, 1986.

[23] Sato K. T., Kane N. L., Soos G., Gisolfi C. V., Kondo N., and Sato K., "Reexamination of tympanic membrane temperature as a core temperature," *J. Appl. Physiol.*, vol. 80, no. 4, pp. 1233-9, 1996.

[24] Kitamura K. I., Zhu X., Chen W. X., and Nemoto T., "Development of a new method for the noninvasive measurement of deep body temperature without a heater," *Med. Eng. Phys.*, vol. 32, no. 1, pp. 1-6, 2010, doi:10.1016/j.medengphy.2009.09.004.

[25] Harasawa K., Kemmotsu O., Mayumi T., and Kawano Y., "Comparison of tympanic, esophageal and blood temperatures during mild hypothermic cardiopulmonary bypass: a study using an infrared emission detection tympanic

thermometer," *J. Clin. Monit.,* vol. 13, no. 1, pp. 19-24, 1997, doi:10.1023/A:1007328005057.

[26] Mariak Z., Lewko J., Luczaj J., Polocki B., and White M. D., "The relationship between directly measured human cerebral and tympanic temperatures during changes in brain temperatures," *Eur. J. Appl. Physiol. Occup. Physiol.,* vol. 69, no. 6, pp. 545-9, 1994, doi:10.1007/Bf00239873.

[27] Shibasaki M., Kondo N., Tominaga H., Aoki K., Hasegawa E., Idota Y., and Moriwaki T., "Continuous measurement of tympanic temperature with a new infrared method using an optical fiber," *J. Appl. Physiol.,* vol. 85, no. 3, pp. 921-6, 1998.

[28] Casa D. J., Becker S. M., Ganio M. S., Brown C. M., Yeargin S. W., Roti M. W., Siegler J., Blowers J. A., Glaviano N. R., and Huggins R. A., "Validity of devices that assess body temperature during outdoor exercise in the heat," *J. Athl. Train.,* vol. 42, no. 3, pp. 333-42, 2007.

[29] Lee J., Matsumura K., Yamakoshi K., Rolfe P., Tanaka N., Yamakoshi Y., Takahashi K., Kim K. H., Hirose H., and Yamakoshi T., "Development of a novel tympanic temperature monitoring system for GT car racing athletes," in *World Congress on Med. Phys. Biomed. Eng. May 26-31, 2012*, Beijing, China, 2013, pp. 2062-5, doi:10.1007/978-3-642-29305-4_541.

[30] Yamakoshi T., Tanaka N., Yamakoshi Y., Matsumura K., Rolfe P., Hirose H., and Takahashi K., "Development of a core body thermometer with built-in earphone for continuous monitoring in GT car racing athletes," *Tran. Jpn. Soc. Med. Biol. Eng.,* vol. 48, no. 5, pp. 494-504, 2010, doi:10.11239/jsmbe.50.227.

[31] Yamakoshi T., Matsumura K., Rolfe P., Tanaka N., Yamakoshi Y., and Takahashi K., "A novel method to detect heat illness under severe conditions by monitoring tympanic temperature," *Aviat. Space Environ. Med.,* vol. 84, no. 7, pp. 692-700, 2013, doi:10.3357/ASEM.3542.2013.

[32] Allen J., "Photoplethysmography and its application in clinical physiological

measurement," *Physiol. Meas.*, vol. 28, no. 3, pp. R1-39, 2007, doi:10.1088/0967-3334/28/3/R01.

[33] Yu C., Liu Z., McKenna T., Reisner A. T., and Reifman J., "A method for automatic identification of reliable heart rates calculated from ECG and PPG waveforms," *J. Am. Med. Inform. Assoc.*, vol. 13, no. 3, pp. 309-20, 2006, doi:10.1197/jamia.M1925.

[34] Brown C. C., Giddon D. B., and Dean E. D., "Techniques of plethysmography," *Psychophysiol.*, vol. 1, no. 3, pp. 253-66, 1965.

[35] Webster J. G., "Measurement of flow and volume of blood," in *Medical instrumentation application and design*, 4th ed., Webster J. G., Ed., United States: John Wiley & Sons, 2009, pp. 338-76.

[36] Challoner A. V. J., "Photoelectric plethysmography for estimating cutaneous blood flow," in *Noninvasive physiological measurements* vol. 1, Rolfe P., Ed., London: Academic Press, 1979, pp. 125-51.

[37] Lopez-Silva S. M., Giannetti R., Dotor M. L., Silveira J. P., Golmayo D., Miguel-Tobal F., Bilbao A., Galindo M., and Martin-Escudero P., "Heuristic algorithm for photoplethysmographic heart rate tracking during maximal exercise test," *J. Med. Biol. Eng.*, vol. 32, no. 3, pp. 181-8, 2012, doi:10.5405/Jmbe.898.

[38] Townshend J., Taylor B. J., Galland B., and Williams S., "Comparison of new generation motion-resistant pulse oximeters," *J. Paediatr. Child Health*, vol. 42, no. 6, pp. 359-65, 2006, doi:10.1111/j.1440-1754.2006.00873.x.

[39] Allen J. and Murray A., "Similarity in bilateral photoplethysmographic peripheral pulse wave characteristics at the ears, thumbs and toes," *Physiol. Meas.*, vol. 21, no. 3, pp. 369-77, 2000, doi:10.1088/0967-3334/21/3/303.

[40] Brodersen O., Römhild D., Starke D., Steinke A., and Vogel S., "In-ear acquisition of vital signs discloses new chances for preventive continuous

cardiovascular monitoring," in *4th Int. workshop on wearable and implantable body sensor networks*, RWTH Aachen University, Germany, 2007, pp. 189-94, doi:10.1007/978-3-540-70994-7_33.

[41] Vogel S., Hulsbusch M., Hennig T., Blazek V., and Leonhardt S., "In-ear vital signs monitoring using a novel microoptic reflective sensor," *IEEE Trans. Inf. Technol. Biomed.*, vol. 13, no. 6, pp. 882-9, 2009, doi:10.1109/TITB.2009.2033268.

[42] Wartzek T., Vogel S., Hennig T., Broderserp O., Hulsbusch M., Herzog M., and Leonhardt S., "Analysis of heart rate variability with an in-ear micro-optic sensor in view of motion artifacts," in *6th Int. Workshop on Wearable and Implantable Body Sensor Networks*, Berkeley, CA, 2009, pp. 168-72, doi:10.1109/bsn.2009.19.

[43] Sawada Y., Tanaka G., and Yamakoshi K., "Normalized pulse volume (NPV) derived photo-plethysmographically as a more valid measure of the finger vascular tone," *Int. J. Psychophysiol.*, vol. 41, no. 1, pp. 1-10, 2001, doi:10.1016/S0167-8760(00)00162-8.

[44] Davis D. L. and Hertzman A. B., "The analysis of vascular reactions in the nasal mucosa with the photoelectric plethysmograph," *Ann. Otol. Rhinol. Laryngol.*, vol. 66, no. 3, pp. 622-40, 1957.

[45] Tanaka G. and Sawada Y., "Examination of normalized pulse volume-blood volume relationship: toward a more valid estimation of the finger sympathetic tone," *Int. J. Psychophysiol.*, vol. 48, no. 3, pp. 293-306, 2003, doi:10.1016/S0167-8760(03)00056-4.

[46] Xin S. Z., Hu S. J., Crabtree V. P., Zheng J., Azorin-Peris V., Echiadis A., and Smith P. R., "Investigation of blood pulse PPG signal regulation on toe effect of body posture and lower limb height," *J. Zhejiang Univ.-Sc. A*, vol. 8, no. 6, pp. 916-20, 2007, doi:10.1631/jzus.2007.A0916.

[47] Allen J. and Murray A., "Age-related changes in the characteristics of the

photoplethysmographic pulse shape at various body sites," *Physiol. Meas.*, vol. 24, no. 2, pp. 297-307, 2003, doi:10.1088/0967-3334/24/2/306.

[48] Matsumura K. and Yamakoshi T., "iPhysioMeter: a new approach for measuring heart rate and normalized pulse volume using only a smartphone," *Behav. Res. Methods.*, vol. 45, no. 4, pp. 1272-8, 2013, doi:10.3758/s13428-012-0312-z.

[49] Nielsen B., "Natural cooling of the brain during outdoor bicycling?," *Pflugers. Arch.*, vol. 411, no. 4, pp. 456-61, 1988.

[50] Deschamps A., Levy R. D., Cosio M. G., Marliss E. B., and Magder S., "Tympanic temperature should not be used to assess exercise induced hyperthermia," *Clin. J. Sport Med.*, vol. 2, no. 1, pp. 27-32, 1992, doi:10.1097/00042752-199201000-00005.

[51] Easton C., Fudge B. W., and Pitsladis Y. P., "Rectal, telemetry pill and tympanic membrane thermometry during exercise heat stress," *J. Therm. Biol.*, vol. 32, no. 2, pp. 78-86, 2007, doi:10.1016/j.jtherbio.2006.10.004.

[52] Cui W. J., Ostrander L. E., and Lee B. Y., "In vivo reflectance of blood and tissue as a function of light wavelength," *IEEE Trans. Biomed. Eng.*, vol. 37, no. 6, pp. 632-9, 1990, doi:10.1109/10.55667.

[53] Maeda Y., Sekine M., and Tamura T., "The advantages of wearable green reflected photoplethysmography," *J. Med. Syst.*, vol. 35, no. 5, pp. 829-34, 2011, doi:10.1007/s10916-010-9506-z.

[54] Maeda Y., Sekine M., and Tamura T., "Relationship between measurement site and motion artifacts in wearable reflected photoplethysmography," *J. Med. Syst.*, vol. 35, no. 5, pp. 969-76, 2011, doi:10.1007/s10916-010-9505-0.

[55] Lee J., Matsumura K., Yamakoshi K. I., Rolfe P., Tanaka S., and Yamakoshi T., "Comparison between red, green and blue light reflection photoplethysmography for heart rate monitoring during motion," in *35th Ann. Int. Conf. IEEE Eng. Med. Biol. Soc. (EMBC)*, Osaka, Japan, 2013, pp. 1724-7,

doi:10.1109/embc.2013.6609852.

[56] Nishimura G., Katayama K., Kinjo M., and Tamura M., "Diffusing-wave absorption spectroscopy in homogeneous turbid media," *Opt. Commun.*, vol. 128, no. 1-3, pp. 99-107, 1996, doi:10.1016/0030-4018(96)00088-0.

[57] Twersky V., "Multiple scattering of waves and optical phenomena," *J. Opt. Soc. Am.*, vol. 52, no. 2, pp. 145-69, 1962, doi:10.1364/JOSA.52.000145.

[58] Twersky V., "Absorption and multiple scattering by biological suspensions," *J. Opt. Soc. Am.*, vol. 60, no. 8, pp. 1084-93, 1970, doi:10.1364/JOSA.60.001084.

[59] Lee J., Matsumura K., Yamakoshi T., Rolfe P., Tanaka N., Kim K., and Yamakoshi K., "Validation of normalized pulse volume in the outer ear as a simple measure of sympathetic activity using warm and cold pressor tests: towards applications in ambulatory monitoring," *Physiol. Meas.*, vol. 34, no. 3, pp. 359-75, 2013, doi:10.1088/0967-3334/34/3/359.

[60] Benzinger T. H., "Heat regulation: homeostasis of central temperature in man," *Physiol. Rev.*, vol. 49, no. 4, pp. 671-759, 1969.

[61] Newsham K. R., Saunders J. E., and Nordin E. S., "Comparison of rectal and tympanic thermometry during exercise," *South. Med. J.*, vol. 95, no. 8, pp. 804-10, 2002.

[62] Kolka M. A., Levine L., and Stephenson L. A., "Use of an ingestible telemetry sensor to measure core temperature under chemical protective clothing," *J. Therm. Biol.*, vol. 22, no. 4-5, pp. 343-9, 1997, doi:10.1016/S0306-4565(97)00032-6.

[63] Bland J. M. and Altman D. G., "Statistical methods for assessing agreement between two methods of clinical measurement," *Lancet*, vol. 1, no. 8476, pp. 307-10, 1986, doi:1016/S0140-6736(86)90837-8.

[64] Moran D. S. and Mendal L., "Core temperature measurement: methods and

current insights," *Sports Med.,* vol. 32, no. 14, pp. 879-85, 2002, doi:0112-1642/02/0014-0879.

[65] Betta V., Cascetta F., and Sepe D., "An assessment of infrared tympanic thermometers for body temperature measurement," *Physiol. Meas.,* vol. 18, no. 3, pp. 215-25, 1997, doi:10.1088/0967-3334/18/3/006.

[66] Robinson J. L., Jou H., and Spady D. W., "Accuracy of parents in measuring body temperature with a tympanic thermometer," *BMC Fam. Pract.,* vol. 6, no. 1, p. 3, 2005, doi:10.1186/1471-2296-6-3.

[67] Lee S. M., Williams W. J., and Fortney Schneider S. M., "Core temperature measurement during supine exercise: esophageal, rectal, and intestinal temperatures," *Aviat. Space Environ. Med.,* vol. 71, no. 9, pp. 939-45, 2000.

[68] O'Brien C., Hoyt R. W., Buller M. J., Castellani J. W., and Young A. J., "Telemetry pill measurement of core temperature in humans during active heating and cooling," *Med. Sci. Sports Exerc.,* vol. 30, no. 3, pp. 468-72, 1998, doi:10.1097/00005768-199803000-00020.

[69] Byrne C. and Lim C. L., "The ingestible telemetric body core temperature sensor: a review of validity and exercise applications," *Br. J. Sports Med.,* vol. 41, no. 3, pp. 126-33, 2007, doi:10.1136/bjsm.2006.026344.

[70] McKenzie J. E. and Osgood D. W., "Validation of a new telemetric core temperature monitor," *J. Therm. Biol.,* vol. 29, no. 7-8, pp. 605-11, 2004, doi:10.1016/j.jtherbio.2004.08.020.

[71] Byrne C., Lee J. K. W., Chew S. A. N., Lim C. L., and Tan E. Y. M., "Continuous thermoregulatory responses to mass-participation distance running in heat," *Med. Sci. Sports Exerc.,* vol. 38, no. 5, pp. 803-10, 2006, doi:10.1249/01.mss.0000218134.74238.6a.

[72] Laursen P. B., Suriano R., Quod M. J., Lee H., Abbiss C. R., Nosaka K., Martin D. T., Bishop D., Sharwood K., and Noakes T., "Core temperature and hydration

status during an Ironman triathlon," *Br. J. Sports Med.,* vol. 40, no. 4, pp. 320-5, 2006, doi:10.1136/bjsm.2005.022426.

[73] Teunissen L. P. J., de Haan A., de Koning J. J., and Daanen H. A. M., "Telemetry pill versus rectal and esophageal temperature during extreme rates of exercise-induced core temperature change," *Physiol. Meas.,* vol. 33, no. 6, pp. 915-24, 2012, doi:10.1088/0967-3334/33/6/915.

[74] Aulick L. H., Robinson S., and Tzankoff S. P., "Arm and leg intravascular temperatures of men during submaximal exercise," *J. Appl. Physiol. Respir. Environ. Exerc. Physiol.,* vol. 51, no. 5, pp. 1092-7, 1981.

[75] Lee J. Y., Nakao K., Takahashi N., Son S. Y., Bakri I., and Tochihara Y., "Validity of infrared tympanic temperature for the evaluation of heat strain while wearing impermeable protective clothing in hot environments," *Ind. Health,* vol. 49, no. 6, pp. 714-25, 2011, doi:10.2486/indhealth.MS1291.

[76] Han H. and Kim J., "Artifacts in wearable photoplethysmographs during daily life motions and their reduction with least mean square based active noise cancellation method," *Comput. Biol. Med.,* vol. 42, no. 4, pp. 387-93, 2012, doi:10.1016/j.compbiomed.2011.12.005.

[77] Spigulis J., Gailite L., Lihachev A., and Erts R., "Simultaneous recording of skin blood pulsations at different vascular depths by multiwavelength photoplethysmography," *Appl. Opt.,* vol. 46, no. 10, pp. 1754-9, 2007, doi:10.1364/AO.46.001754.

[78] Lindberg L. G. and Oberg P. A., "Photoplethysmography. part 2. Influence of light source wavelength," *Med. Biol. Eng. Comput.,* vol. 29, no. 1, pp. 48-54, 1991, doi:10.1007/BF02446295.

[79] Anderson R. R. and Parrish J. A., "The optics of human skin," *J. Invest. Dermatol.,* vol. 77, no. 1, pp. 13-9, 1981, doi:10.1111/1523-1747.ep12479191.

[80] Kohen E., Santus R., and Hirschberg J. G., "Optical properties of the skin," in

Photobiology, United Kingdom, London: Academic Press, 1995, pp. 303-22.

[81] Giltvedt J., Sira A., and Helme P., "Pulsed multifrequency photoplethysmograph," *Med. Biol. Eng. Comput.*, vol. 22, no. 3, pp. 212-5, 1984, doi:10.1007/BF02442745.

[82] Ugnell H. and Oberg P. A., "The time-variable photoplethysmographic signal; dependence of the heart synchronous signal on wavelength and sample volume," *Med. Eng. Phys.*, vol. 17, no. 8, pp. 571-8, 1995, doi:10.1016/1350-4533(95)00008-B.

[83] Neuman M. R., "Biopotential amplifiers," in *Medical instrumentation application and design*, 4th ed., Webster J. G., Ed., United States: John Wiley & Sons, 2009, pp. 241-92.

[84] Foulds I. S., "Organ structure and function: the skin," in *Occupational hygiene*, 3rd ed., Gardiner K. and Harrington J. M., Eds., United Kingdom, Oxford: Blackwell Publishing Ltd, 2008, pp. 25-35, doi:10.1002/9780470755075.ch4.

[85] Muldoon M. F., Bachen E. A., Manuck S. B., Waldstein S. R., Bricker P. L., and Bennett J. A., "Acute cholesterol responses to mental stress and change in posture," *Arch. Intern. Med.*, vol. 152, no. 4, pp. 775-80, 1992, doi:10.1001/archinte.1992.00400160079015.

[86] Allen M. T., Shelley K. S., and Boquet A. J., Jr., "A comparison of cardiovascular and autonomic adjustments to three types of cold stimulation tasks," *Int. J. Psychophysiol.*, vol. 13, no. 1, pp. 59-69, 1992, doi:10.1016/0167-8760(92)90021-3.

[87] Allen M. T., Matthews K. A., and Sherman F. S., "Cardiovascular reactivity to stress and left ventricular mass in youth," *Hypertens.*, vol. 30, no. 4, pp. 782-7, 1997, doi:10.1161/01.HYP.30.4.782.

[88] Saab P. G., Llabre M. M., Hurwitz B. E., Schneiderman N., Wohlgemuth W., Durel L. A., Massie C., and Nagel J., "The cold pressor test: vascular and

myocardial response patterns and their stability," *Psychophysiol.,* vol. 30, no. 4, pp. 366-73, 1993, doi:10.1111/j.1469-8986.1993.tb02058.x.

[89] Uretzky G. and Palti Y., "A method for comparing transmitted and reflected light photoelectric plethysmography," *J. Appl. Physiol.,* vol. 31, no. 1, pp. 132-5, 1971.

[90] Nijboer J. A., Dorlas J. C., and Mahieu H. F., "Photoelectric plethysmography some fundamental aspects of the reflection and transmission method," *Clin. Phys. Physiol. Meas.,* vol. 2, no. 3, pp. 205-215, 1981, doi:10.1088/0143-0815/2/3/004.

[91] Matsumura K., Yamakoshi T., Noguchi H., Rolfe P., and Matsuoka Y., "Fish consumption and cardiovascular response during mental stress," *BMC Res. Notes,* vol. 5, p. 288, 2012, doi:10.1186/1756-0500-5-288.

[92] Miller S. B. and Ditto B., "Individual differences in heart rate and peripheral vascular responses to an extended aversive task," *Psychophysiol,* vol. 26, no. 5, pp. 506-513, 1989, doi:10.1111/j.1469-8986.1989.tb00703.x.

[93] Miller S. B. and Ditto B., "Exaggerated sympathetic nervous system response to extended psychological stress in offspring of hypertensives," *Psychophysiol,* vol. 28, no. 1, pp. 103-113, 1991, doi:10.1111/j.1469-8986.1991.tb03395.x.

[94] Panerai R. B., "Assessment of cerebral pressure autoregulation in humans-a review of measurement methods," *Physiol. Meas.,* vol. 19, no. 3, pp. 305-38, 1998, doi:10.1088/0967-3334/19/3/001.

[95] Matsumura K., Yamakoshi T., Yamakoshi Y., and Rolfe P., "The effect of competition on heart rate during kart driving: a field study," *BMC Res. Notes,* vol. 4, p. 342, 2011, doi:10.1186/1756-0500-4-342.

[96] Yamakoshi T., Matsumura K., Yamakoshi Y., Hirose H., and Rolfe P., "Physiological measurements and analyses in motor sports: a preliminary study in racing kart athletes," *Eur. J. Sport. Sci.,* vol. 10, no. 6, pp. 397-406, 2010, doi:10.1080/17461391003699112.